Cell

Programmed Translational Readthrough Generates Antiangiogenic VEGF-Ax

Sandeepa M. Eswarappa,[1] Alka A. Potdar,[1,2] William J. Koch,[1] Yi Fan,[1,6] Kommireddy Vasu,[1] Daniel Lindner,[3] Belinda Willard,[4] Linda M. Graham,[5] Paul E. DiCorleto,[1] and Paul L. Fox[1,*]
[1]Department of Cellular and Molecular Medicine, The Lerner Research Institute, Cleveland Clinic, Cleveland, OH 44195, USA
[2]Department of Biomedical Engineering, Case Western Reserve University, Cleveland, OH 44106, USA
[3]Taussig Cancer Center, Cleveland Clinic, Cleveland, OH 44195, USA
[4]Mass Spectrometry Laboratory for Protein Sequencing, The Lerner Research Institute, Cleveland Clinic, Cleveland, OH 44195, USA
[5]Department of Biomedical Engineering, The Lerner Research Institute, Cleveland Clinic, Cleveland, OH 44195, USA
[6]Present address: Department of Radiation Oncology, University of Pennsylvania Perelman School of Medicine, Philadelphia, PA 19104, USA
*Correspondence: foxp@ccf.org
http://dx.doi.org/10.1016/j.cell.2014.04.033

SUMMARY

Translational readthrough, observed primarily in less complex organisms from viruses to *Drosophila*, expands the proteome by translating select transcripts beyond the canonical stop codon. Here, we show that vascular endothelial growth factor A (*VEGFA*) mRNA in mammalian endothelial cells undergoes programmed translational readthrough (PTR) generating VEGF-Ax, an isoform containing a unique 22-amino-acid C terminus extension. A *cis*-acting element in the *VEGFA* 3′ UTR serves a dual function, not only encoding the appended peptide but also directing the PTR by decoding the UGA stop codon as serine. Heterogeneous nuclear ribonucleoprotein (hnRNP) A2/B1 binds this element and promotes readthrough. Remarkably, VEGF-Ax exhibits antiangiogenic activity in contrast to the proangiogenic activity of VEGF-A. Pathophysiological significance of VEGF-Ax is indicated by robust expression in multiple human tissues but depletion in colon adenocarcinoma. Furthermore, genome-wide analysis revealed *AGO1* and *MTCH2* as authentic readthrough targets. Overall, our studies reveal a novel protein-regulated PTR event in a vertebrate system.

INTRODUCTION

Vascular endothelial growth factor A (VEGF-A) induces migration and proliferation in vascular endothelial cells (ECs) and is essential for both physiological (e.g., embryogenesis) and pathological (e.g., tumorigenesis, retinopathy, and arthritis) angiogenesis (Ferrara, 2009; Hicklin and Ellis, 2005; Nagy et al., 2007). ECs not only respond to VEGF-A but also express and secrete it, and EC-derived VEGF-A exhibits an intracellular activity essential for vascular homeostasis (Lee et al., 2007). VEGF-A also increases vascular permeability (Senger et al., 1983) and is required for maintenance of the differentiated phenotype in ECs (Kamba et al., 2006). Deletion of the *VEGFA* gene, even at a single allele, or a 2-fold increase of VEGF-A is embryonic lethal, demonstrating a precise VEGF-A dosage requirement during development (Carmeliet et al., 1996; Ferrara et al., 1996; Miquerol et al., 2000). VEGF-A functions primarily through two tyrosine kinase receptors, VEGFR1 (or flt-1) and VEGFR2 (or KDR or flk-1), and neuropilin 1 serves as an important coreceptor (Soker et al., 1998). Because VEGF-A is critical for the pathogenesis of vascularized solid tumors, agents that selectively target the protein, receptor, or signaling pathway have received substantial attention. As an example, bevacizumab, a monoclonal antibody that targets human VEGF-A, is an FDA-approved drug successfully used to treat metastatic colorectal cancer (Hurwitz et al., 2004).

The *VEGFA* gene on human chromosome 6 comprises eight exons. Alternative splicing events at the sixth and seventh exons, which encode heparin-binding motifs, generate multiple isoforms, all of which exhibit proangiogenic activity. Interestingly, an alternative splicing event within exon 8 has been reported to generate an antiangiogenic isoform, termed VEGF-Ab (Bates et al., 2002; Harper and Bates, 2008). The splicing event in *VEGFAb* mRNA replaces an exon encoding CDKPRR at the C terminus of canonical proangiogenic isoforms with SLTRKD (RLTRKD in *B. taurus*). VEGF-A expression is regulated by multiple posttranscriptional mechanisms, primarily involving the unusually long 3′ UTR. Heterogeneous nuclear ribonucleoprotein (hnRNP) L binds a CA-rich element, promoting *VEGFA* mRNA stability under hypoxia (Shih and Claffey, 1999). VEGF-A expression is also subject to exquisite translational control mechanisms. In one well-studied example, interferon-γ stimulation of myeloid cells induces binding of the heterotetrameric GAIT (interferon-γ-activated inhibitor of translation) complex to a cognate element in the *VEGFA* 3′ UTR and inhibits its translation (Mazumder et al., 2003; Sampath et al., 2004). A protein-directed RNA switch integrates disparate signals induced by hypoxia and interferon-γ to further regulate *VEGFA* translation expression in myeloid cells (Ray et al., 2009). Interestingly, a mechanism that prevents complete translational silencing of *VEGFA* mRNA has been reported that forces a "trickle" of synthesis, underscoring

the requirement for precise regulation of VEGF-A dosage in physiological conditions (Yao et al., 2012). In addition, *VEGFA* mRNA is subject to 5′ UTR-mediated regulation in which an internal ribosomal entry site drives alternative translation-initiation from an in-frame CUG codon (Huez et al., 2001).

Translation of mRNAs normally terminates at an in-frame stop codon. However, in a few circumstances, translation can continue beyond the stop codon to a downstream stop codon, generating a C-terminal polypeptide extension. Such translational readthrough events are best understood in viruses (Li and Rice, 1989; Pelham, 1978), but translational readthrough has also been observed in bacteria (Jalajakumari et al., 1989), yeast (Namy et al., 2003), and *Drosophila* (Dunn et al., 2013; Robinson and Cooley, 1997; Steneberg and Samakovlis, 2001). In a few systems translational readthrough is ''programmed'' by *cis*-acting RNA elements downstream of the first stop codon, clearly distinguishing the process from readthrough resulting from errors of translation (Firth et al., 2011). Limited evidence for readthrough of vertebrate mRNAs has been shown, namely, rabbit β-globin in rabbits and rat myelin protein zero; however, the functional significance of the readthrough products and the *cis*-acting RNA signals or other regulatory mechanisms have not been determined (Chittum et al., 1998; Yamaguchi et al., 2012). Moreover, to our knowledge, *trans*-acting protein factors that bind RNA elements or otherwise regulate translational readthrough have not been observed.

Here, we demonstrate that *VEGFA* mRNA undergoes robust programmed translational readthrough (PTR) in mammalian ECs. The PTR event generates a VEGF-A isoform, termed VEGF-Ax (for ''extended''), with a 22-amino-acid C terminus extension. Remarkably, VEGF-Ax exhibits a function opposite to that of VEGF-A, namely, antiangiogenic activity. Readthrough is ''programmed'' by a 63 nt RNA segment following the canonical stop codon that serves a dual function, encoding the peptide extension of VEGF-A and also acting as a *cis*-acting regulatory element. hnRNP A2/B1 binds this element and promotes readthrough. The presence of VEGF-Ax in blood and its selective expression in multiple tissues, as well as differential expression in a solid tumor, indicate its pathophysiological significance. Recombinant VEGF-Ax reduced tumor progression and associated angiogenesis in a human xenograft tumor implanted in nude mice, demonstrating its antiangiogenic property in vivo. We have expanded the generality of our findings by a genome-wide analysis that reveals additional validated readthrough targets, namely, *AGO1* and *MTCH2* mRNAs. Overall, our results not only demonstrate a novel PTR event in a vertebrate transcript but also identify a new antiangiogenic isoform of VEGF-A with a potential role as a suppressor of pathological angiogenesis.

RESULTS

Endothelial Cells Express and Secrete an Antiangiogenic Isoform of VEGF-A

Despite recent studies of the autocrine function of EC-derived VEGF-A in blood vessel angiogenesis and homeostasis (da Silva et al., 2010; Lee et al., 2007), its paracrine function has not received much attention. We hypothesized that secreted, EC-derived VEGF-A might be an important contributor to EC migration and proliferation, which are essential for endothelial wound-healing responses and angiogenesis (Ausprunk and Folkman, 1977; Schwartz et al., 1978). Unexpectedly, a VEGF-A-neutralizing antibody enhanced migration of bovine aortic ECs as indicated by the number of migrating cells in a razor-wound assay, as well as by root-mean-square displacement and mean cell speed (Figure 1A). Likewise, the antibody increased EC proliferation determined fluorimetrically as total cell DNA (Figure 1B). Consistent with these observations, addition of EC-conditioned medium decreased EC migration (Figure 1C). These surprising results indicate that EC-derived VEGF-A inhibits their own migration and proliferation, characteristic features of antiangiogenic VEGF-A isoforms. To test for the possible expression of VEGF-Ab isoforms, we sequenced 74 *VEGFA* cDNA clones from bovine aortic ECs (and six from mouse aortic ECs) but did not find VEGF-Ab-specific mRNA or any alternatively spliced *VEGFA* mRNA that can generate antiangiogenic isoforms. Instead, we identified only mRNAs corresponding to proangiogenic VEGF-A_{164} and VEGF-A_{120} (Figures S1A–S1C available online). Similarly, VEGF-Ab-specific mRNA was not detected by RT-PCR using primers designed to differentiate between VEGF-Ab and VEGF-A isoforms (Figure S1D).

VEGF-Ax Is a Novel Isoform Generated by Translational Readthrough of *VEGFA* mRNA

The paradoxical presence of antiangiogenic VEGF-A in the absence of VEGF-Ab-specific mRNA suggested the possibility of a novel antiangiogenic VEGF-A isoform generated from mRNA encoding the proangiogenic isoform. A critical clue was offered by the sequence of the *VEGFA* mRNA 3′ UTR. In the human *VEGFA* 3′ UTR, we observed an evolutionarily conserved UGA stop codon 63 nt downstream and in frame to the canonical stop codon (Figure 1D). Importantly, a 4 nt insertion in rodent 3′ UTRs is offset by a 1 nt deletion, thereby preserving the in-frame nature of the stop codons. Moreover, a mutation in the downstream rodent stop codon generates the alternate UAA stop codon, providing additional evolutionary support for the significance of the in-frame stop codon. The amino acid sequence potentially encoded by the region between the stop codons is likewise conserved in mammals, but the sequence beyond the downstream stop codon exhibits weak conservation (Figures S1E and S1F). Based on these observations, we hypothesized that *VEGFA* mRNA translation might extend beyond its canonical stop codon, terminating at the downstream, in-frame stop codon. This translational readthrough event in human or bovine cells would generate a VEGF-A isoform containing a 22-amino-acid C terminus extension (including an amino acid replacement of the stop codon) ending with S/RLTRKD, the same six-amino-acid terminus reported to confer antiangiogenic activity in human VEGF-Ab (Figure 1E).

To test this hypothesis, we generated an antibody against the unique peptide, AGLEEGASLRVSGTR, generated by the proposed translational readthrough event and not present in VEGF-Ab or any other protein (or in silico-translated mRNA). A 20 kDa protein corresponding to the predicted size of the readthrough product, designated VEGF-Ax (for extended), was identified in lysates from bovine ECs (Figure 2A). Expression was inhibited by transfection with three different *VEGFA*-specific small interfering

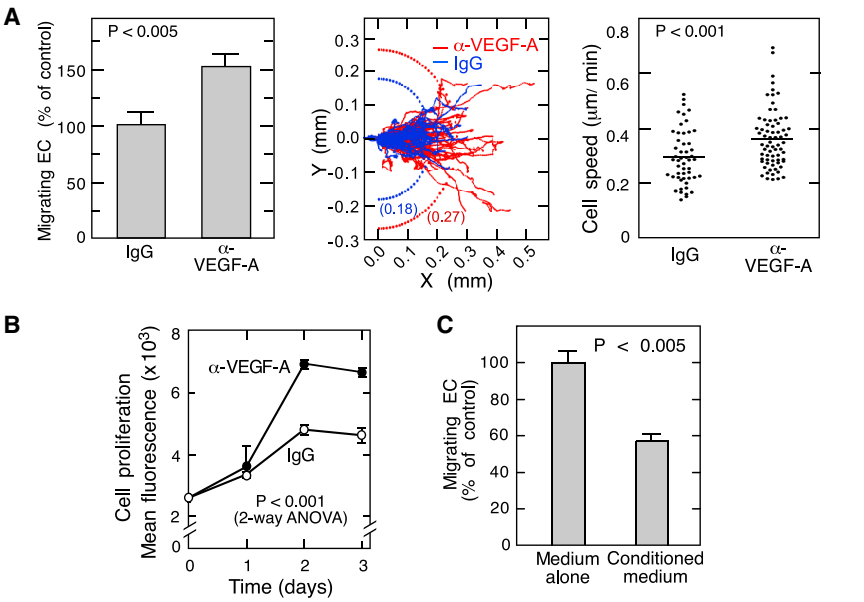

Figure 1. ECs Express and Secrete an Anti-angiogenic Isoform of VEGF-A

(A) Neutralizing anti-VEGF-A antibody enhances EC migration. Shown are ECs migrating across razor-wound line (mean ± SE, n = 3) (left), individual cell trajectories and root-mean-square displacement (center), and cell speed in the presence of anti-VEGF-A antibody (n = 71) and immunoglobulin G (n = 52) (right).

(B) Neutralizing anti-VEGF-A antibody increases EC proliferation. Cell amount was determined fluorimetrically as DNA (mean ± SE, n = 4).

(C) EC-derived conditioned medium inhibits EC migration. EC migration determined by razor-wound assay (mean ± SE, n = 3).

(D) Conservation of *VEGFA* 3′ UTR proximal region (gray); canonical and downstream, in-frame stop codons in mammals (boxed).

(E) Schematic showing generation of VEGF-A, VEGF-Ab, and VEGF-Ax isoforms.

See also Figure S1.

RNAs (siRNAs), consistent with a VEGF-A isoform. Protein immunoprecipitated with anti-VEGF-Ax antibody was recognized by an anti-VEGF-A antibody that targets the N terminus, further verifying VEGF-Ax as a VEGF-A isoform (Figure 2B). To validate antibody specificity, human embryonic kidney 293 (HEK293) cells were transfected with myc-tagged *VEGFA* cDNA up to the downstream stop codon in which the canonical stop codon was replaced by Ala-encoding GCA to ensure efficient generation of the modified, extended isoform, denoted VEGF-Ax^{Ala}. Anti-VEGF-Ax antibody recognized VEGF-Ax^{Ala}, but not VEGF-A, whereas anti-VEGF-A antibody recognized both isoforms (Figure S2A). As expected, anti-VEGF-Ax antibody did not recognize recombinant VEGF-Ab; however, anti-VEGF-Ab antibody did recognize VEGF-Ax^{Ala} (Figure S2B). Finally, preadsorption of anti-VEGF-Ax antibody with AGLEEGASLRVSGTR peptide prevented recognition of the 20 kDa VEGF-Ax band, further validating antibody specificity (Figure S2C). VEGF-Ax expression also was observed in murine aortic and human umbilical vein ECs (Figure 2C) and in multiple other cell types including macrophages, hepatocytes, keratinocytes, and tumor-derived cell lines (Figure S2D). To distinguish between VEGF-Ax and VEGF-A by protein molecular weight, EC lysates were deglycosylated, subjected to 16% Tricine gel electrophoresis, and immunoblotted with anti-VEGF-A and anti-VEGF-Ax antibodies. VEGF-Ax constitutes about 10% of all VEGF-A isoforms in EC lysates; however, VEGF-Ax is the predominant isoform in conditioned medium, constituting about 85% of the total (Figure 2D).

Translational readthrough in *VEGFA* mRNA was further established by mass spectrometric analysis of the product generated by overexpressing in HEK293 cells *VEGFA* cDNA containing the canonical stop codon and the Ax-specific sequence upstream of a myc-His tag to facilitate purification. In addition to detection of VEGF-A-specific peptides, selected reaction monitoring revealed a spectrum consistent with RSAGLEEGASLR (S, Ser in place of stop codon) specific for the readthrough region; the profile was confirmed by the spectrum obtained from synthetic RSAGLEEGASLR peptide (Figures 2E–2G). Spectra consistent with Ser in place of the stop codon were observed in three out of three independent experiments. Targeted search for potential

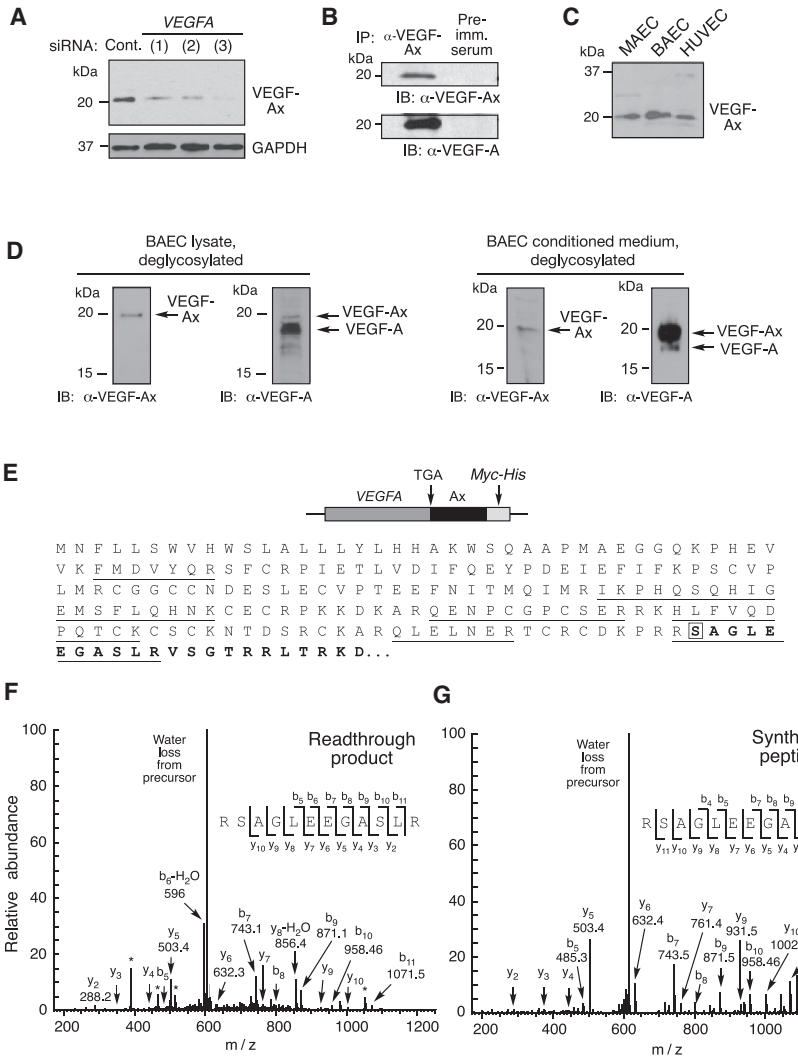

Figure 2. VEGF-Ax Is a Novel Isoform of *VEGFA* Generated by Translational Readthrough

(A) *VEGFA*-specific siRNAs inhibit VEGF-Ax expression. Bovine ECs were transfected with three different *VEGFA*-specific siRNAs and VEGF-Ax in cell lysates determined by immunoblot with anti-VEGF-Ax antibody.

(B) VEGF-Ax is an authentic VEGF-A isoform. Lysates from bovine EC were immunoprecipitated with anti-VEGF-Ax antibody or preimmune (Pre-imm.) serum and subjected to immunoblot analysis with anti-VEGF-Ax and anti-VEGF-A antibodies.

(C) VEGF-Ax is expressed by murine aortic ECs (MAEC), bovine aortic ECs (BAEC), and human umbilical vein ECs (HUVEC). Cell lysates were subjected to immunoblot analysis with anti-VEGF-Ax antibody.

(D) Separation of VEGF-Ax and VEGF-A isoforms in ECs. BAEC lysates (left) and conditioned media (right) were deglycosylated and resolved on 16% Tricine gel before immunoblot analysis with anti-VEGF-Ax and anti-VEGF-A antibodies.

(E) Amino acid sequence of VEGF-Ax. Peptides identified by mass spectrometry (underline), readthrough region (bold), and recoded Ser (boxed) are highlighted.

(F) Identification of *VEGFA* mRNA readthrough product by tandem mass spectrometry (MS/MS). A MS/MS spectrum was identified consistent with RSAGLEEGASLR (readthrough amino acid is underlined). The spectrum contains a total of nine C-terminal "y" ions and seven N-terminal "b" ions consistent with this sequence. The peptide was a low-abundant component, and the spectrum contains several contaminant ions (*).

(G) Identity of readthrough peptide validated by synthetic peptide. RSAGLEEGASLR peptide was synthesized and the MS/MS spectrum determined as in (F).

See also Figure S2.

readthrough peptides containing the other 19 amino acids in place of the stop codon was negative, supporting Ser insertion during UGA stop codon readthrough.

Ax Element Is the Necessary and Sufficient *cis*-Acting Signal for Translational Readthrough of *VEGFA* mRNA

To validate translation readthrough and investigate molecular mechanisms, we established a reporter assay in which the full-length bovine *VEGFA* coding sequence (corresponding to VEGF-A_{164}) up to and including the 63 nt, Ax-specific sequence (termed Ax element) was cloned upstream of and in frame with firefly luciferase *(FLuc)*. The downstream stop codon was excluded so that readthrough at the canonical stop codon generated a FLuc-containing chimeric protein. Transfected ECs exhibited substantially greater FLuc activity compared to vector alone or control reporters lacking the Ax element or replaced by a nonspecific sequence, consistent with translation readthrough (Figure 3A). To calculate readthrough efficiency, the upstream TGA stop codon was mutated to Ala-encoding GCA to maximize FLuc expression; stop codon readthrough efficiency was about 9%. Quantitative RT-PCR (qRT-PCR) analysis showed that all constructs were transcribed at similar levels, indicating that differential FLuc activity was due to differences in translation. Similar results were obtained by in vitro translation of the same reporters in rabbit reticulocyte lysates (Figure S3A). These results verify translational readthrough in *VEGFA* mRNA and show the essentiality of the Ax element, consistent with a PTR mechanism.

To investigate if the Ax element drives readthrough in the context of a heterologous transcript, a construct was engineered containing *Myc* terminated with a TGA stop codon, upstream and in frame to the Ax element and *FLuc* (*Myc*-Ax-*FLuc*). Transfection into ECs induced substantial FLuc activity compared to a control transcript without the Ax element or empty vector (Figure 3B, left). The readthrough product was detected following immunoprecipitation using anti-Myc-tag antibody by immunoblot (Figure 3B, right) and by mass spectrometry (Figure S3B). Also, Ax element-mediated readthrough of *Myc*-Ax-*FLuc* was

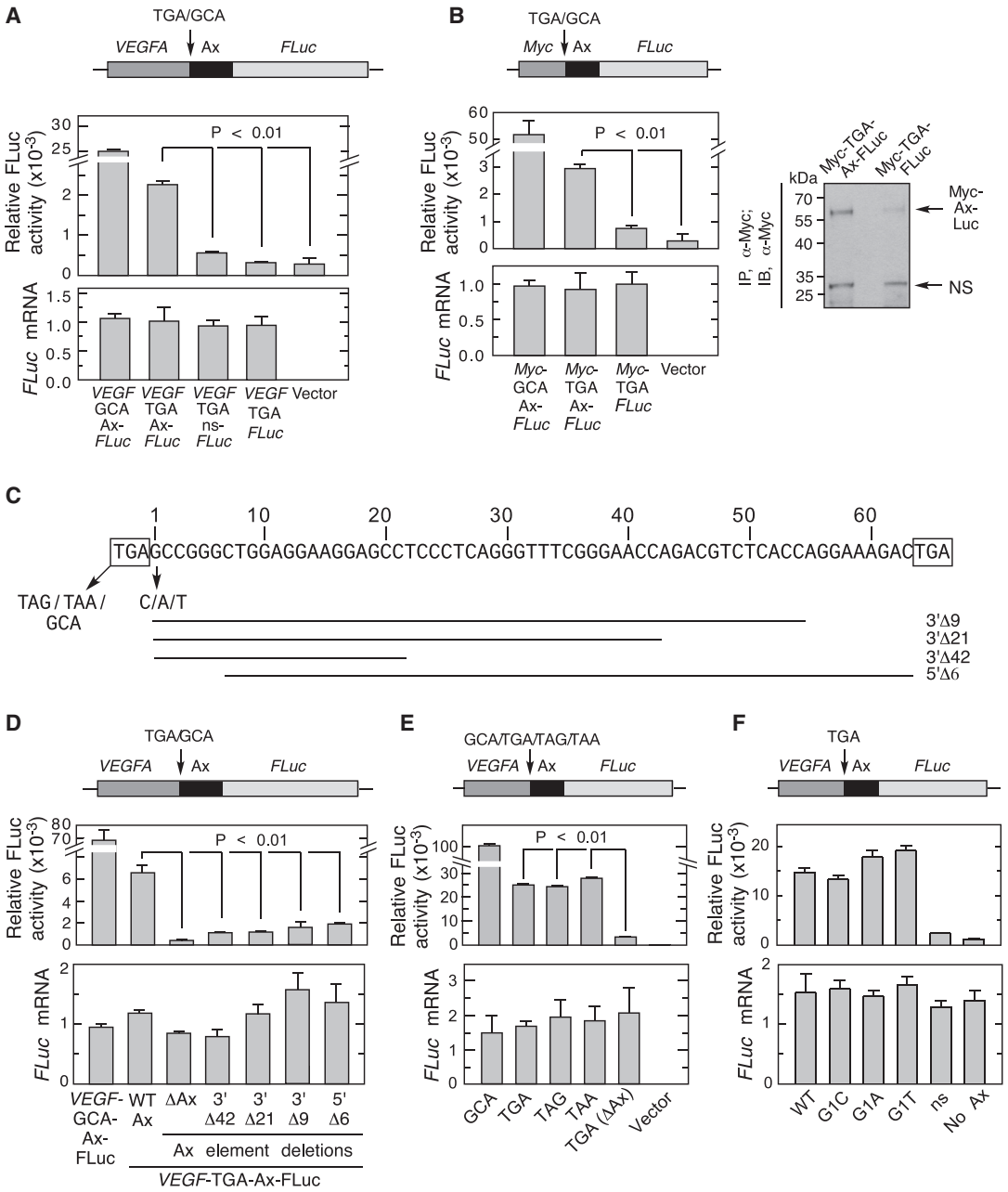

Figure 3. Ax Element Is a Necessary and Sufficient *cis*-Acting Signal for *VEGFA* mRNA Readthrough

(A) Ax element is sufficient for readthrough of *VEGFA* chimeric transcript. Plasmid containing in-frame *VEGF*-Ax-*FLuc*, and variants with TGA-to-GCA substitution, no Ax element, and Ax replaced by a nonspecific sequence (ns), were transfected into ECs. FLuc activity was normalized to expression of cotransfected *Renilla Luc* (top), and *FLuc* mRNA expression was determined by qRT-PCR (bottom).

(B) Ax element is sufficient for readthrough of heterologous mRNA. Chimeric plasmids containing *Myc*-Ax-*FLuc* and variants were transfected into ECs. Relative FLuc activity and mRNA expression were measured (left). Readthrough product also was determined by immunoprecipitation with rabbit anti-Myc-tag antibody followed by immunoblot with the mouse anti-Myc-tag antibody (right).

(C) Nucleotide sequence of bovine Ax element. Flanking stop codons (boxes), deletions (horizontal lines), and mutations (arrows) are shown.

(D) Plasmids containing deletions of *VEGF*-Ax-*FLuc* were transfected into ECs. FLuc activity was normalized by expression of cotransfected *Renilla Luc* (top); *FLuc* mRNA expression was determined by qRT-PCR (bottom).

(E) All three stop codons permit readthrough. ECs were transfected with *VEGF*-Ax-*FLuc* constructs containing each stop codon. Relative FLuc activity and mRNA were determined.

(F) The nucleotide immediately following the canonical stop codon (G1) does not alter readthrough efficiency. ECs were transfected with *VEGF*-Ax-*FLuc* constructs containing G-to-C, G-to-A, and G-to-T substitutions. Relative FLuc activity and mRNA were measured.

For all graphs, error bars represent SE; n = 3. See also Figure S3.

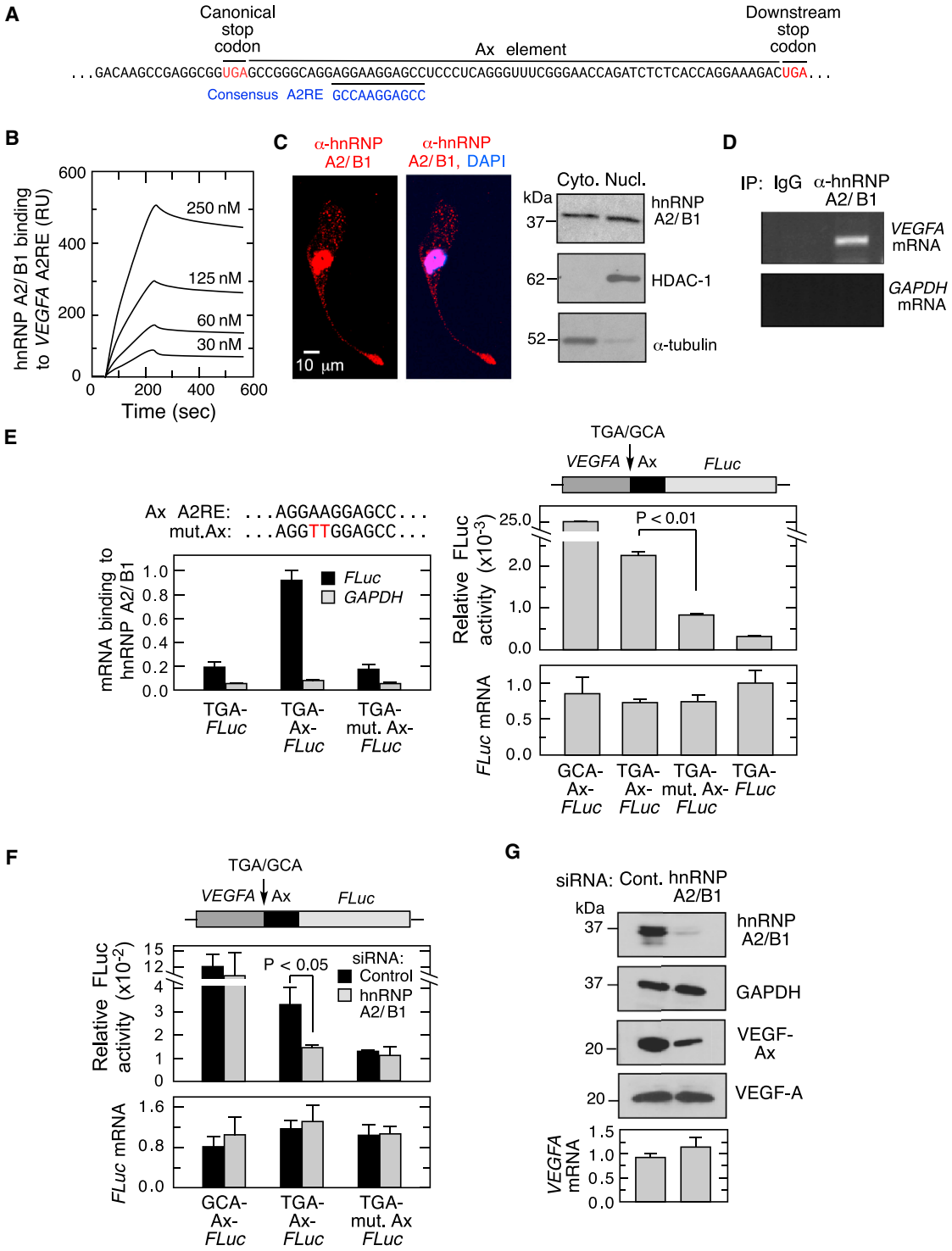

Figure 4. hnRNP A2/B1 Facilitates *VEGFA* mRNA Translational Readthrough

(A) Interstop codon sequence (Ax element) of human *VEGFA* contains a near-consensus hnRNP A2/B1 response element (A2RE).

(B) High-affinity binding of hnRNP A2/B1 to *VEGFA* A2RE. Surface plasmon resonance analysis of recombinant hnRNP A2/B1 binding to biotinylated RNA containing *VEGFA* A2RE immobilized on streptavidin sensor chip (in response units [RU]).

(C) Cytoplasmic localization of hnRNP A2/B1 in ECs. Detection of hnRNP A2/B1 by immunofluorescence (left, with nuclear DAPI stain) and by immunoblot of fractionated compartments (right). Cyto., cytoplasm; Nucl., nucleus.

(D) hnRNP A2/B1 binds *VEGFA* mRNA in cells. Immunoprecipitation of hnRNP A2/B1 followed by RT-PCR using *VEGFA*- and *GAPDH*-specific primers.

(legend continued on next page)

shown by in vitro translation in rabbit reticulocyte lysate (Figure S3C). To determine the region of the Ax element necessary for function, deletions from both termini were generated (Figure 3C). Deletion of 9, 21, or 42 nt from the 3′ end or 6 nt from the 5′ end substantially reduced FLuc activity, suggesting that both termini are required, and possibly the entire element, for efficient readthrough (Figure 3D). Next, we tested the ability of Ax element to execute readthrough across the other two stop codons, UAG and UAA. Surprisingly, similar Ax element-mediated *VEGFA* readthrough was observed across all three stop codons (Figure 3E), thereby rejecting single stop codon-dependent mechanisms, such as UGA-dependent selenocysteine insertion (Low and Berry, 1996). Mutation of the first nucleotide after the canonical stop codon (denoted G1) did not affect the readthrough efficiency, ruling out context-dependent readthrough mechanisms observed in other systems (Poole et al., 1995; Tate et al., 1999) (Figure 3F). Together, these experiments reveal the Ax element as the necessary and sufficient translational readthrough signal in *VEGFA* mRNA.

hnRNP A2/B1 Is a *trans*-Acting Enhancer of *VEGFA* Readthrough

A near-consensus hnRNP A2/B1 recognition element (A2RE) was identified within the Ax element (Figure 4A). hnRNP A2/B1 is an RNA-binding protein involved in pre-mRNA processing and mRNA transport and binds the consensus sequence 5′-GCCAAGGAGCC-3′ (He and Smith, 2009; Shan et al., 2003). Surface plasmon resonance spectroscopy revealed a high-affinity interaction between hnRNP A2/B1 and a *VEGFA* RNA segment containing the A2RE, with a dissociation constant (K_D) of 19.2 ± 5.6 nM (Figure 4B). hnRNP A2/B1 is localized primarily in the nucleus; however, cytoplasmic localization was detected by immunofluorescence and by fractionation (Figure 4C). An RNA-binding protein immunoprecipitation (RIP) experiment confirmed the intracellular interaction between endogenous hnRNP A2/B1 and *VEGFA* mRNA (Figure 4D). To interrogate interaction specificity, ECs were transfected with a *FLuc* reporter bearing wild-type, mutant (AA-to-TT), or no Ax element. RIP followed by qRT-PCR analysis showed that hnRNP A2/B1 interacted with the wild-type Ax element, but not with the mutant element (Figure 4E, left) (Munro et al., 1999). Mutation of the A2RE also substantially reduced readthrough without altering mRNA expression (Figure 4E, right). The low-level readthrough in the absence of hnRNP A2/B1 binding suggests that other factors might contribute, consistent with the requirement for the entire Ax element, not just the A2RE. Similarly, siRNA-mediated knockdown of hnRNP A2/B1 in ECs reduced readthrough of the *VEGFA*-Ax-*FLuc* reporter without inhibiting FLuc activity of a construct with Ala-encoding GCA in place of the canonical stop codon or with mutant Ax element (Figure 4F). Finally, hnRNP A2/B1 knockdown reduced endogenous expression of VEGF-Ax without affecting total VEGF-A protein or mRNA in ECs (Figure 4G). These observations show the important regulatory role of hnRNP A2/B1 as a *trans*-acting factor promoting PTR of *VEGFA* mRNA.

VEGF-Ax Exhibits Antiangiogenic Properties

Our EC migration and proliferation experiments in the presence of VEGF-A antibody indicated secretion of an antiangiogenic isoform of VEGF-A. Canonical VEGF-A isoforms were not detected in EC-conditioned medium immunodepleted with anti-VEGF-Ax antibody, confirming that VEGF-Ax is the predominant isoform secreted by ECs (Figure S4A). Also, the presence of RLTRKD (and absence of CDKPRR) at the C terminus suggests that VEGF-Ax is a novel antiangiogenic isoform. Anti-VEGF-Ax antibody increased EC migration and proliferation to an extent comparable to induction by recombinant VEGF-A, consistent with a paracrine, antiangiogenic activity of endogenous VEGF-Ax (Figures 5A and 5B; Figure S4B). Purified, recombinant His-VEGF-Ax^{Ala} markedly inhibited planar EC migration, tube formation in Matrigel, and proliferation (Figures 5C–5E). Similarly, siRNA-mediated knockdown of hnRNP A2/B1, which reduces VEGF-Ax production, stimulated EC migration (Figure S4C). Together, these results indicate that VEGF-Ax is the predominant isoform of VEGF-A released by ECs, exerting a potent paracrine, antiangiogenic activity. To obtain insights into the mechanism of action of VEGF-Ax, we investigated its binding to VEGF receptors using solid-phase enzyme-linked receptor-binding assays. His-VEGF-Ax^{Ala} and VEGF-A bound VEGFR2, with comparable affinities, but maximal binding of the former was marginally lower at high ligand concentration (Figure 5F). Importantly, His-VEGF-Ax^{Ala} did not bind neuropilin 1, a critical VEGFR2 coreceptor (Figure 5G). Likewise, His-VEGF-Ax^{Ala} did not trigger canonical signaling pathways as shown by the failure to phosphorylate VEGFR2 Tyr residues Y1175 and Y951 (Figure 5H).

Pathophysiological Significance of VEGF-Ax

To determine the antiangiogenic function of VEGF-Ax in vivo, we used human xenograft tumors in nude mice. Administration of recombinant VEGF-Ax markedly reduced the progression of HCT116 (human colon carcinoma cell)-derived tumors (Figure 6A). Furthermore, VEGF-Ax reduced tumor-associated angiogenesis as measured by the number of vessels directly feeding the tumors (Figure 6B). To further assess the physiological significance of VEGF-Ax, we determined its expression in vivo using a tissue microarray. VEGF-Ax was detected in tissue slices from human brain, colon, small intestine, spleen, and pancreas and from serum from healthy human subjects (Figures S5A and S5B). Staining of human colon tissue with

(E) hnRNP A2/B1 binds the A2RE in *VEGFA* mRNA. *VEGF*-Ax-*FLuc* plasmid containing an Ax element with A2RE mutation (mut. Ax) was transfected into ECs. Anti-hnRNP A2/B1 immunoprecipitates were probed by qRT-PCR using *FLuc*- and *GAPDH*-specific TaqMan probes (left). Readthrough expressed as relative FLuc activity and mRNA level are shown (right).

(F) siRNA-mediated knockdown of hnRNP A2/B1 reduces readthrough of Ax element-containing plasmid. ECs were transfected with *VEGF*-Ax-*FLuc* construct and the variant containing A2RE mutation. FLuc activity was measured and *FLuc* mRNA determined by qRT-PCR.

(G) siRNA-mediated knockdown of hnRNP A2/B1 reduces VEGF-Ax expression. Following siRNA-mediated knockdown of hnRNP A2/B1, VEGF-Ax and VEGF-A were determined by immunoblot analysis and *VEGFA* mRNA by qRT-PCR.

For all graphs, error bars represent SE; n = 3.

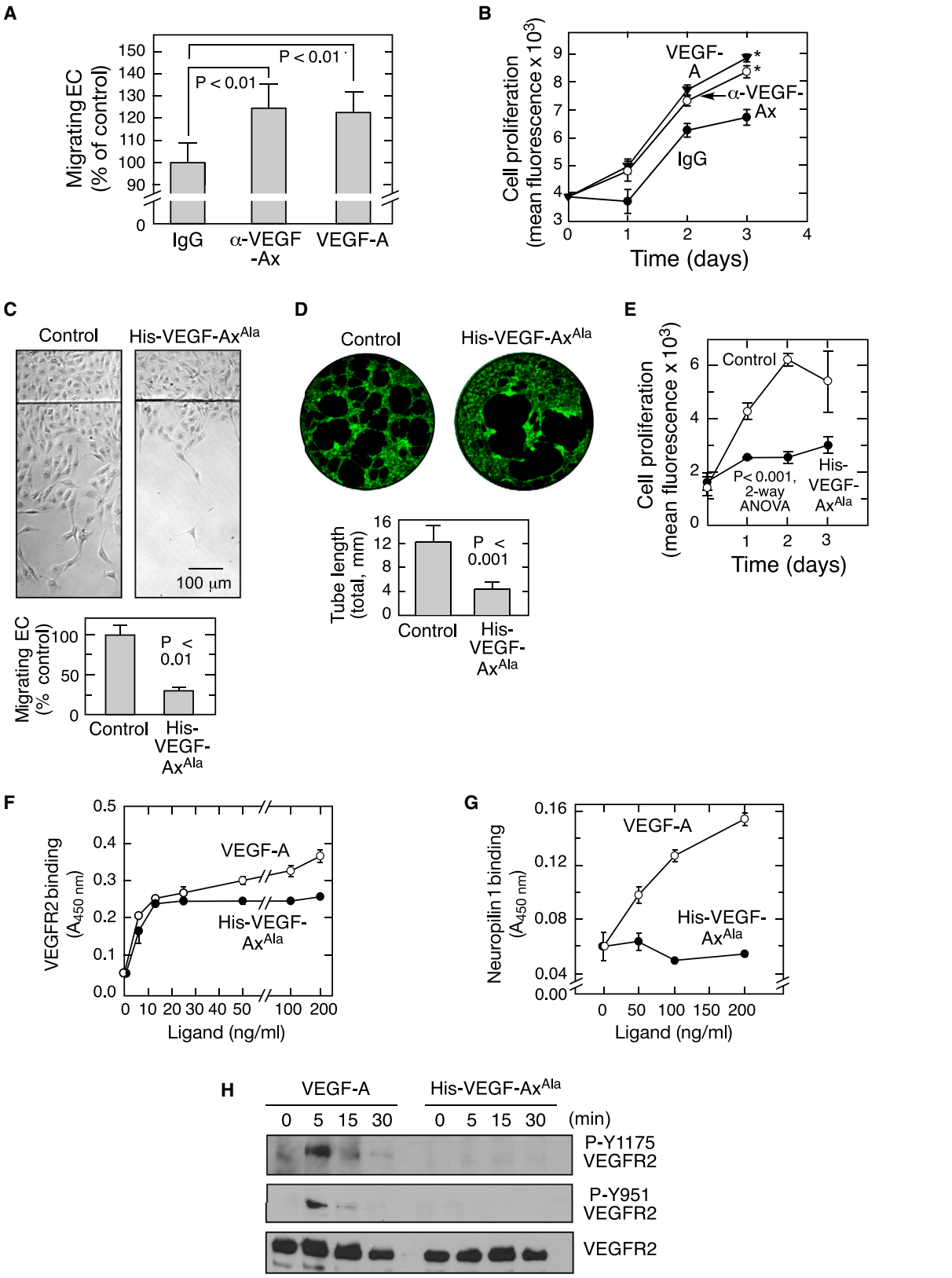

(legend on next page)

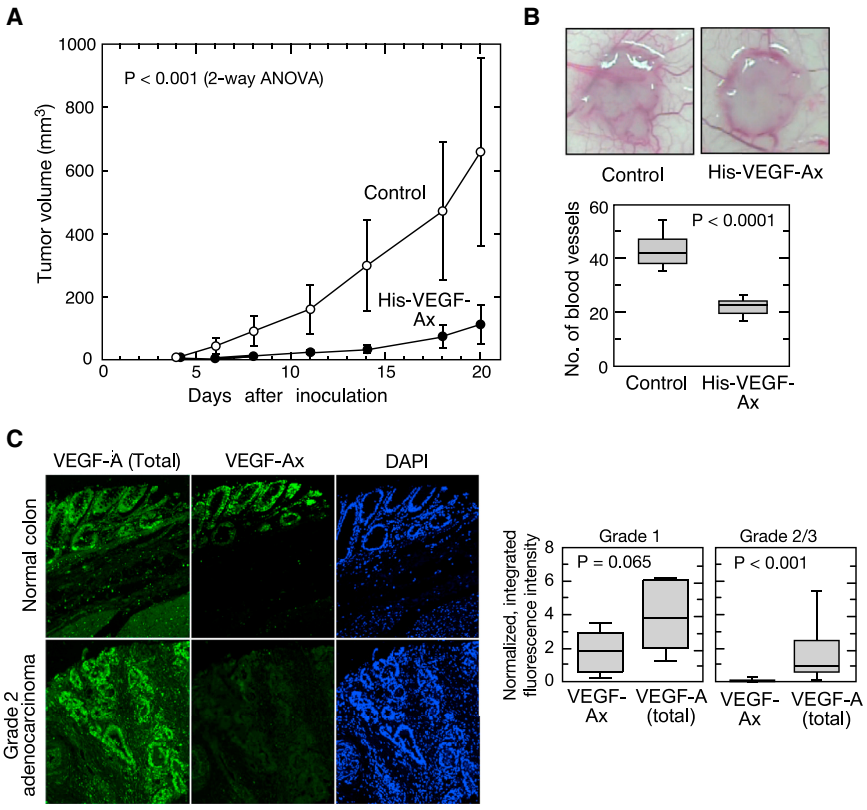

Figure 6. Antitumor Properties of VEGF-Ax

(A) Tumor progression in athymic nude mice. Mice were inoculated with HCT116 cells and treated subcutaneously with recombinant His-VEGF-Ax (10 μg/mouse; n = 6 mice, 12 tumors) or buffer (n = 5 mice, 10 tumors) every third day starting from fourth day after tumor cell inoculation.

(B) Tumor angiogenesis. Representative images of day 6 HCT116 tumors in athymic nude mice (top). Number of blood vessels feeding directly into tumors; whiskers show 5th and 95th percentiles (bottom; n = 6 mice, 12 tumors in each group).

(C) Immunofluorescence of normal colon and colon adenocarcinoma. VEGF-Ax and total VEGF-A were quantified as integrated, background-subtracted fluorescence intensity (left); expression in grade 1 (n = 6) and grade 2/3 colon adenocarcinoma (n = 22) was normalized to healthy colon (n = 5); whiskers show 5th and 95th percentiles (right).

See also Figure S5.

anti-VEGF-Ax antibody preadsorbed with AGLEEGASLRVSGTR peptide showed only background signal demonstrating antibody specificity in tissue immunofluorescence assays (Figure S5C). VEGF-Ax expression in tissues from pancreatic adenocarcinoma and glioblastoma was similar to that in corresponding healthy tissues (data not shown). Remarkably, VEGF-Ax expression was reduced to near-background level in cancerous tissues from grade 2 or 3 adenocarcinoma of colon, despite abundant VEGF-A expression (Figure 6C). These results not only show that VEGF-A translational readthrough occurs in vivo but also suggest a possible negative role of VEGF-Ax in tumor progression.

Genome-wide Analysis of Translational Readthrough

To identify additional translational readthrough candidates in mammals, we performed a genome-wide bioinformatic analysis. We interrogated a UTR database (Grillo et al., 2010) for mammalian transcripts with a stop codon in the 3′ UTR in frame to the canonical stop codon and with amino acid conservation in the interstop codon region across five mammalian species (Figure S6). This screen revealed *VEGFA* and five high-probability readthrough candidates (Figure 7A). Candidates were tested by transfection of HEK293 cells with a plasmid containing about 700 nt of the 3′ terminus of the human coding sequence of each candidate, followed by the interstop codon sequence and *FLuc*. *MTCH2* and *AGO1* showed robust readthrough activity (Figure 7B). Readthrough efficiency was determined by comparison to corresponding in-frame control constructs where UGA stop codon is replaced with Ala-encoding GCA. Readthrough efficiency for *VEGFA*, *MTCH2*, and *AGO1* was calculated to be 11%, 13%, and ~24%, respectively.

DISCUSSION

Organisms have evolved a plethora of mechanisms at multiple levels to expand their proteomes relative to their surprisingly limited number of distinct genes. Among the most employed examples are alternative splicing and alternative polyadenylation at the posttranscriptional level, alternative initiation at the translational level, and protein cleavage and modification at the posttranslational level. There are multiple examples, but little mechanistic information about proteome expansion by translational readthrough that can generate proteins with extended

Figure 5. Antiangiogenic Properties of VEGF-Ax

(A and B) Anti-VEGF-Ax antibody increases EC migration and proliferation. (A) EC migration in the presence of anti-VEGF-Ax antibody or recombinant human VEGF-A (20 ng/ml) was measured by razor-wound assay. (B) Cell proliferation was measured fluorimetrically as DNA (*p < 0.05, two-way ANOVA).

(C–E) Antiangiogenic properties of VEGF-Ax. Migration (C), tube formation in Matrigel (D), and proliferation (E) of bovine ECs in the presence of recombinant His-VEGF-Ax^{ala} (50 ng/ml).

(F and G) Binding of VEGF-A and His-VEGF-Ax^{ala} to VEGFR2 (F) and neuropilin 1 (G). Binding was measured colorimetrically by solid-phase enzyme-linked receptor-binding assay.

(H) Phosphorylation status of VEGFR2. HUVECs were treated with VEGF-A and His-VEGF-Ax^{Ala} for up to 30 min and immunoblotted as shown.

For all graphs, error bars represent SE; n = 3. See also Figure S4.

A

Gene name	Function	Alignment score	Stop codons (*Homo sapiens*)		
			Canonical	Downstream	Distance between stops (nt)
AGO1	Argonaute 1, RNA interference	2310	UGA	UAG	99
MTCH2	Mitochondrial carrier protein	1463	UGA	UAG	30
NR1D1	Transcriptional repressor	3389	UGA	UGA	144
ADAMTS4	Cleaves aggrecan	2088	UAA	UAG	45
TOX	Unknown (T-cell development?)	2611	UGA	UAG	117
VEGFA	Angiogenesis	2015	UGA	UGA	63

B

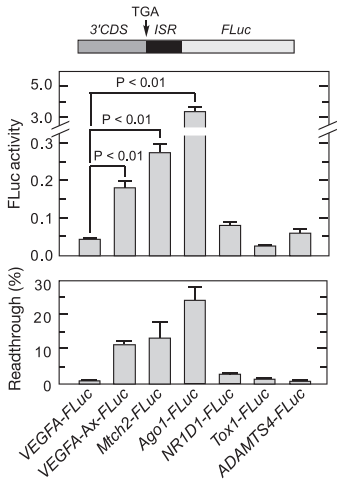

Figure 7. Genome-wide Analysis to Identify Targets of Translational Readthrough

(A) Properties of candidate genes selected for experimental validation. Candidates were selected using a bioinformatic screening protocol (Figure S6).

(B) Validation of translational readthrough targets. Chimeric plasmids containing about 700 nt of the 3′ terminus of human coding sequences (3′CDS) upstream of the interstop codon region (ISR) and in frame with *FLuc* were transfected into HEK293 cells. Relative FLuc activities normalized to *FLuc* mRNA were determined by qRT-PCR (top). Readthrough efficiency is expressed as percent of FLuc activity of normal translation controls in which canonical UGA stop codon is replaced by GCA (bottom). For all graphs, error bars represent SE; n = 3.

See also Figure S6.

C termini and potentially with alternate functions compared to the shorter, canonical form. Although some mechanistic insights have been provided by studies of translational readthrough in RNA viruses, little is known about mechanisms of translational readthrough in vertebrates and its role in proteome expansion. Here, we reveal a PTR event in *VEGFA* transcript that generates an antiangiogenic isoform, VEGF-Ax. Readthrough events have been described in vertebrate transcripts, for example, rabbit β-globin and rat myelin protein zero (Chittum et al., 1998; Yamaguchi et al., 2012), and a recent ribosome profiling experiment provided evidence for translational readthrough of 42 mRNAs in human fibroblasts (Dunn et al., 2013). However, the functional significance of the readthrough product has not been shown in any of these cases.

Basal readthrough levels ranging from 0.02% to 1.4% have been observed in yeast and mammalian cells (Dunn et al., 2013). In viruses, where multiple readthrough events have been established, 6% efficiency in murine leukemia virus (MLV) and 2%–5% in *Sindbis* have been reported (Houck-Loomis et al., 2011; Li and Rice, 1989). In these cases, the nucleotide sequence downstream of the canonical stop codon serves as a signal directing readthrough, establishing them as authentic programmed events unambiguously distinguishable from translation errors (Firth et al., 2011; Rajon and Masel, 2011). For example, a 63 nt RNA element downstream of the stop codon induces translational readthrough in the MLV *gag-pol* gene (Houck-Loomis et al., 2011). In our studies, the readthrough efficiency of *VEGFA* ranges from 7% to 25%. *VEGFA* mRNA readthrough is programmed by the Ax element, a 63-nt-long RNA sequence between the two stop codons that can drive readthrough in a heterologous system. We also identify hnRNP A2/B1 as a *trans*-factor that binds the A2RE in the Ax element and positively regulates *VEGFA* readthrough. This finding is particularly noteworthy in that regulation of translational readthrough by a *trans*-factor has not been reported.

Although context-specific regulation of readthrough is suggested by a ribosome profiling study that showed differential readthrough of nine transcripts in two *Drosophila* cell types (Dunn et al., 2013), molecular mechanisms underlying such regulation have not been elucidated in any system. As one possible mechanism, we speculate that the Ax element, in coordination with hnRNP A2/B1, interacts directly or indirectly (e.g., by inducing a pause) with the translating ribosomes and prevents eukaryotic releasing factor 1 (eRF1) binding to the stop codon. As a consequence, the UGA stop codon could instead be recognized by a suppressor tRNA or by near-cognate tRNAs resulting in readthrough. This mechanism is supported by several observations: (1) protein interactome studies suggest that hnRNP A2/B1 interacts with several ribosomal proteins, including S7, S19, S28, L27a, and L39 (Havugimana et al., 2012; Kristensen et al., 2012); (2) ribosome occupancy is asymmetric at the stop codon, occupying 6 nt downstream of the stop codon (Ingolia et al., 2009). The A2RE element starts at the 11th nt following the stop codon, possibly facilitating an interaction between hnRNP A2/B1 and a ribosome paused at the stop codon, (3) aminoglycosides, which induce readthrough, also bind ribosomes (Howard et al., 2004; Kondo et al., 2005), and (4) the observed readthrough of all three stop codons suggests that a single tRNA species may not be involved. A deep mechanistic understanding to the readthrough mechanism might require structural studies of the relationship of the Ax element and its binding partner with the paused ribosome.

Serine was identified as the amino acid inserted in the place of the UGA codon during *VEGFA* mRNA readthrough. Interestingly, the tRNA that inserts selenocysteine (Sec) in place of UGA codons, namely tRNA$^{[Ser]Sec}$, specifically recognizes UGA codons and is initially charged with Ser before it is phosphorylated and converted to Sec by Sec synthase (Turanov et al., 2011). Moreover, Ser-tRNA$^{[Ser]Sec}$ can suppress termination at a UGA codon in rabbit β-globin mRNA in vitro (Chittum et al., 1998; Diamond et al., 1981). Thus, Ser-tRNA$^{[Ser]Sec}$ is a candidate for Ser insertion during *VEGFA* mRNA readthrough. Alternatively, a Ser-tRNA^{Ser} can contribute to readthrough as a consequence of compromised ribosome fidelity. Although only Ser was identified in place of the UGA codon of *VEGFA* mRNA, other amino acids might be inserted; Trp, Cys, and

Arg are likely candidates, as they have been observed in other readthrough events involving the UGA stop codon, namely, in rabbit β-globin (Chittum et al., 1998) and *gag-pol* MLV (Feng et al., 1990). However, these and other amino acids likely constitute a minor fraction, as they were not observed even after targeted mass spectrometry analysis. The observed readthrough across all stop codon types was unexpected, but nonsense suppression across all three stop codons has been reported in mammalian systems (Beier and Grimm, 2001; Hatfield et al., 1990). Recognition of all three stop codons by eRF1 is also consistent with our finding of promiscuous readthrough (Kisselev et al., 2003).

Translational readthrough contributes significantly to the proteome expansion in yeast, *Drosophila*, and human fibroblasts (Dunn et al., 2013; Jungreis et al., 2011; von der Haar and Tuite, 2007). Using a bioinformatic, genome-wide approach based on evolutionary conservation of the intrastop codon sequence, we have identified five additional putative readthrough targets, none of which have been previously described. Translational readthrough was experimentally validated in two mRNAs, *AGO1* and *MTCH2*. MTCH2 induces apoptosis by recruiting tBID (truncated BH3-interacting domain death agonist) to mitochondria (Zaltsman et al., 2010); *AGO1* (or *EIF2C1*) encodes Argonaute 1, an important participant in the microRNA and RNAi systems (Kim et al., 2006). Although the other candidates (*NR1D1*, *TOX1*, and *ADAMTS4*) were inactive in our luciferase-based readthrough assay in HEK293 cells, they might be readthrough targets in other conditions or cells. The *AGO1* and *MTCH2* 3′ UTRs do not share sequence similarity with the Ax element, nor do they possess an A2RE, suggesting that their readthrough mechanisms are likely to be different from that of *VEGFA* mRNA.

The concept of antiangiogenic VEGF-A isoforms was introduced by the report of an alternative splicing event within the terminal exon of *VEGFA* to generate *VEGFAb* mRNA that replaces CDKPRR at the C terminus with SLTRKD, conferring antiangiogenic properties in vitro (Bates et al., 2002). Several laboratories have shown that recombinant or overexpressed VEGF-Ab inhibits in vivo angiogenesis in murine tumor models, in mammary tissue of transgenic mice, and during neovascularization in mouse retina, rabbit cornea, and rat mesentery (Cébe Suarez et al., 2006, 2008; Cromer et al., 2010; Konopatskaya et al., 2006; Manetti et al., 2011; Qiu et al., 2008; Rennel et al., 2008, 2009; Woolard et al., 2004). Lastly, immunological evidence for robust VEGF-Ab expression has been reported in multiple cells and tissues (Harper and Bates, 2008). Despite these promising observations, the in vivo expression of VEGF-Ab remains controversial, based in part on the observation that the RT-PCR methods used for detection and quantitation are prone to error (Bates et al., 2013; Harris et al., 2012). Similarly, we were unable to detect *VEGFAb* mRNA isoforms in ECs despite robust expression of antiangiogenic activity. At present, detection by anti-VEGF-Ab antibody is considered the strongest support for expression of endogenous VEGF-Ab. However, this evidence is confounded by the presence of the same SLTRKD hexapeptide at the C termini in both VEGF-Ax and VEGF-Ab, and anti-VEGF-Ab antibodies raised against this region do not distinguish between the two isoforms. In contrast, the antibody raised against the first 15 amino acids of the peptide extension of VEGF-Ax is highly specific for VEGF-Ax (Figure S2B). New tools and approaches are required to resolve the relative in vivo expression of the various pro- and antiangiogenic isoforms. Development of antibodies that recognize VEGF-Ab, but not VEGF-Ax, possibly by targeting the junction of the sequence encoded by exon 7 and SLTRKD, would be extremely helpful. Also, RNA sequencing analysis could not only provide strong support for expression of *VEGFAb* isoforms but also offer insight into the relative amounts of differentially spliced *VEGFA* and *VEGFAb* isoforms in a given tissue or cell type.

VEGF-Ax exhibits potent antiangiogenic activity as evidenced by inhibition of EC migration, proliferation, and tube formation in vitro and tumor growth and associated angiogenesis in vivo. A report of enhanced EC sprouting in aortic rings from mice heterozygous for EC-specific *VEGFA* gene deletion (da Silva et al., 2010) is consistent with our finding of predominant antiangiogenic VEGF-Ax in EC-conditioned medium. The discovery of antiangiogenic VEGF-A isoforms compels a need for cognizance and caution in applying VEGF-A-targeted therapies for treatment of VEGF-A-dependent malignancies, as coincident diminution of VEGF-Ax may exacerbate angiogenesis and tumorigenesis (Harper and Bates, 2008; Varey et al., 2008). Moreover, usefulness of VEGF-A as a biomarker might also need to be reconsidered in the view of potential presence of both pro- and antiangiogenic isoforms. We speculate that expression of VEGF-Ax is an innate mechanism that evolved to limit EC movement and angiogenesis during tissue homeostasis and to reduce pathological angiogenesis. However, in some conditions exemplified by colon adenocarcinoma in our study, a loss of expression of VEGF-Ax might induce angiogenesis and exacerbate pathogenesis. Thus, abnormally low levels of VEGF-Ax in plasma or tissues can serve as a biomarker for prognosis or effective susceptibility to current anti-VEGF treatment. Moreover, because of its robust antiangiogenic activity, VEGF-Ax provides a potential therapeutic agent against diseases characterized by excessive angiogenesis.

EXPERIMENTAL PROCEDURES

Cell Culture

Bovine aortic ECs were cultured in Dulbecco's modified Eagle's medium (DMEM)/Ham's F-12 medium containing 5% fetal bovine serum (FBS) and used in all experiments unless specified otherwise. Human umbilical vein ECs (HUVECs) were cultured in EC growth medium with SingleQuots supplements (Lonza). HEK293 cells were cultured in DMEM containing 10% FBS. Cells were maintained at 37°C in a humidified atmosphere with 5% CO_2.

Luciferase-Based Translational Readthrough Assay

Plasmids containing chimera of FLuc downstream of test sequences (*VEGFA*, *Myc*, *TOX*, *ADAMTS4*, *AGO1*, *NR1D1*, or *MTCH2*) were transfected (500 ng/well) into bovine ECs or HEK293 cells in 24-well plates using Lipofectamine 2000. Plasmid expressing Renilla luciferase (RLuc) (50 ng/well) was cotransfected as efficiency control. After 48 hr, cells were lysed and FLuc and RLuc activity were measured using Dual-Luciferase Reporter Assay System (Promega) in a Victor3 1420 Multilabel Plate Counter (Perkin-Elmer). The same constructs were subjected to in vitro coupled transcription-translation (500 ng/reaction) using TNT T7 coupled rabbit reticulocyte lysates (Promega) and FLuc activity measured by Luciferase Assay System (Promega).

Animal Studies

Nu/Nu athymic nude male mice were inoculated subcutaneously on both flanks with HCT116 human colon carcinoma cells. Mice were injected subcutaneously with His-VEGF-Ax (10 μg/mouse) obtained from HEK293 cells stably expressing bovine VEGF-Ax with Ser in place of the canonical stop codon. HiTrap Heparin HP Columns (GE Healthcare) were used for purification. Control mice were injected with buffer containing 25 mM Tris and 150 mM NaCl (pH 8). Injections were given every third day starting from the fourth day after tumor inoculation. Tumor progression was monitored by caliper determination of volume [(shortest diameter)^2 × (longest diameter) × 0.525]. For determination of tumor angiogenesis, treatment was started on the second day after tumor inoculation, and blood vessels feeding directly into day 6 tumors were counted under a dissecting microscope at 12.5× magnification. Images were captured using PSMT5 operating microscope (World Precision) with 12.5 × objective lens; every visible vessel touching the circumference of the tumor nodule was scored as a single vessel by an observer blinded to the treatment. Animal studies were conducted under the oversight of Animal Research Committee of the Cleveland Clinic. Animals were housed in the animal facility of Cleveland Clinic accredited by the Association and Accreditation of Laboratory Animal Care.

For further detail, please see Extended Experimental Procedures.

SUPPLEMENTAL INFORMATION

Supplemental Information includes Extended Experimental Procedures and six figures and can be found with this article online at http://dx.doi.org/10.1016/j.cell.2014.04.033.

ACKNOWLEDGMENTS

This work was supported in part by NIH grants P01 HL029582, P01 HL076491, R01 GM086430, R01 DK083359, and R21 HL094841 (to P.L.F.). S.M.E. was supported by a fellowship from the American Heart Association, Great Rivers Affiliate. A shared instrument grant (S10 RR031537) from the NIH (to B.W.) was used to purchase the Orbitrap mass spectrometer. Mouse studies were supported by the Athymic Animal and Xenograft Core, NCI P30 CA043703-23, of the Case Comprehensive Cancer Center (to D.L.). We are grateful to Donna Driscoll and Jodi Bubenik for helpful discussions. S.M.E. and P.L.F. are inventors on a patent that has been filed related to this work.

Received: December 13, 2013
Revised: February 21, 2014
Accepted: April 4, 2014
Published: June 19, 2014

REFERENCES

Ausprunk, D.H., and Folkman, J. (1977). Migration and proliferation of endothelial cells in preformed and newly formed blood vessels during tumor angiogenesis. Microvasc. Res. *14*, 53–65.

Bates, D.O., Cui, T.G., Doughty, J.M., Winkler, M., Sugiono, M., Shields, J.D., Peat, D., Gillatt, D., and Harper, S.J. (2002). VEGF165b, an inhibitory splice variant of vascular endothelial growth factor, is down-regulated in renal cell carcinoma. Cancer Res. *62*, 4123–4131.

Bates, D.O., Mavrou, A., Qiu, Y., Carter, J.G., Hamdollah-Zadeh, M., Barratt, S., Gammons, M.V., Millar, A.B., Salmon, A.H., Oltean, S., and Harper, S.J. (2013). Detection of VEGF-A(xxx)b isoforms in human tissues. PLoS ONE *8*, e68399.

Beier, H., and Grimm, M. (2001). Misreading of termination codons in eukaryotes by natural nonsense suppressor tRNAs. Nucleic Acids Res. *29*, 4767–4782.

Carmeliet, P., Ferreira, V., Breier, G., Pollefeyt, S., Kieckens, L., Gertsenstein, M., Fahrig, M., Vandenhoeck, A., Harpal, K., Eberhardt, C., et al. (1996). Abnormal blood vessel development and lethality in embryos lacking a single VEGF allele. Nature *380*, 435–439.

Cébe Suarez, S., Pieren, M., Cariolato, L., Arn, S., Hoffmann, U., Bogucki, A., Manlius, C., Wood, J., and Ballmer-Hofer, K. (2006). A VEGF-A splice variant defective for heparan sulfate and neuropilin-1 binding shows attenuated signaling through VEGFR-2. Cell. Mol. Life Sci. *63*, 2067–2077.

Cébe-Suarez, S., Grünewald, F.S., Jaussi, R., Li, X., Claesson-Welsh, L., Spillmann, D., Mercer, A.A., Prota, A.E., and Ballmer-Hofer, K. (2008). Orf virus VEGF-E NZ2 promotes paracellular NRP-1/VEGFR-2 coreceptor assembly via the peptide RPPR. FASEB J. *22*, 3078–3086.

Chittum, H.S., Lane, W.S., Carlson, B.A., Roller, P.P., Lung, F.D., Lee, B.J., and Hatfield, D.L. (1998). Rabbit beta-globin is extended beyond its UGA stop codon by multiple suppressions and translational reading gaps. Biochemistry *37*, 10866–10870.

Cromer, W., Jennings, M.H., Odaka, Y., Mathis, J.M., and Alexander, J.S. (2010). Murine rVEGF164b, an inhibitory VEGF reduces VEGF-A-dependent endothelial proliferation and barrier dysfunction. Microcirculation *17*, 536–547.

da Silva, R.G., Tavora, B., Robinson, S.D., Reynolds, L.E., Szekeres, C., Lamar, J., Batista, S., Kostourou, V., Germain, M.A., Reynolds, A.R., et al. (2010). Endothelial alpha3beta1-integrin represses pathological angiogenesis and sustains endothelial-VEGF. Am. J. Pathol. *177*, 1534–1548.

Diamond, A., Dudock, B., and Hatfield, D. (1981). Structure and properties of a bovine liver UGA suppressor serine tRNA with a tryptophan anticodon. Cell *25*, 497–506.

Dunn, J.G., Foo, C.K., Belletier, N.G., Gavis, E.R., and Weissman, J.S. (2013). Ribosome profiling reveals pervasive and regulated stop codon readthrough in Drosophila melanogaster. eLife *2*, e01179.

Feng, Y.X., Copeland, T.D., Oroszlan, S., Rein, A., and Levin, J.G. (1990). Identification of amino acids inserted during suppression of UAA and UGA termination codons at the gag-pol junction of Moloney murine leukemia virus. Proc. Natl. Acad. Sci. USA *87*, 8860–8863.

Ferrara, N. (2009). Vascular endothelial growth factor. Arterioscler. Thromb. Vasc. Biol. *29*, 789–791.

Ferrara, N., Carver-Moore, K., Chen, H., Dowd, M., Lu, L., O'Shea, K.S., Powell-Braxton, L., Hillan, K.J., and Moore, M.W. (1996). Heterozygous embryonic lethality induced by targeted inactivation of the VEGF gene. Nature *380*, 439–442.

Firth, A.E., Wills, N.M., Gesteland, R.F., and Atkins, J.F. (2011). Stimulation of stop codon readthrough: frequent presence of an extended 3′ RNA structural element. Nucleic Acids Res. *39*, 6679–6691.

Grillo, G., Turi, A., Licciulli, F., Mignone, F., Liuni, S., Banfi, S., Gennarino, V.A., Horner, D.S., Pavesi, G., Picardi, E., and Pesole, G. (2010). UTRdb and UTRsite (RELEASE 2010): a collection of sequences and regulatory motifs of the untranslated regions of eukaryotic mRNAs. Nucleic Acids Res. *38*, D75–D80.

Harper, S.J., and Bates, D.O. (2008). VEGF-A splicing: the key to anti-angiogenic therapeutics? Nat. Rev. Cancer *8*, 880–887.

Harris, S., Craze, M., Newton, J., Fisher, M., Shima, D.T., Tozer, G.M., and Kanthou, C. (2012). Do anti-angiogenic VEGF (VEGFxxxb) isoforms exist? A cautionary tale. PLoS ONE *7*, e35231.

Hatfield, D.L., Smith, D.W., Lee, B.J., Worland, P.J., and Oroszlan, S. (1990). Structure and function of suppressor tRNAs in higher eukaryotes. Crit. Rev. Biochem. Mol. Biol. *25*, 71–96.

Havugimana, P.C., Hart, G.T., Nepusz, T., Yang, H., Turinsky, A.L., Li, Z., Wang, P.I., Boutz, D.R., Fong, V., Phanse, S., et al. (2012). A census of human soluble protein complexes. Cell *150*, 1068–1081.

He, Y., and Smith, R. (2009). Nuclear functions of heterogeneous nuclear ribonucleoproteins A/B. Cell. Mol. Life Sci. *66*, 1239–1256.

Hicklin, D.J., and Ellis, L.M. (2005). Role of the vascular endothelial growth factor pathway in tumor growth and angiogenesis. J. Clin. Oncol. *23*, 1011–1027.

Houck-Loomis, B., Durney, M.A., Salguero, C., Shankar, N., Nagle, J.M., Goff, S.P., and D'Souza, V.M. (2011). An equilibrium-dependent retroviral mRNA switch regulates translational recoding. Nature *480*, 561–564.

Howard, M.T., Anderson, C.B., Fass, U., Khatri, S., Gesteland, R.F., Atkins, J.F., and Flanigan, K.M. (2004). Readthrough of dystrophin stop codon mutations induced by aminoglycosides. Ann. Neurol. *55*, 422–426.

Huez, I., Bornes, S., Bresson, D., Créancier, L., and Prats, H. (2001). New vascular endothelial growth factor isoform generated by internal ribosome entry site-driven CUG translation initiation. Mol. Endocrinol. *15*, 2197–2210.

Hurwitz, H., Fehrenbacher, L., Novotny, W., Cartwright, T., Hainsworth, J., Heim, W., Berlin, J., Baron, A., Griffing, S., Holmgren, E., et al. (2004). Bevacizumab plus irinotecan, fluorouracil, and leucovorin for metastatic colorectal cancer. N. Engl. J. Med. *350*, 2335–2342.

Ingolia, N.T., Ghaemmaghami, S., Newman, J.R., and Weissman, J.S. (2009). Genome-wide analysis in vivo of translation with nucleotide resolution using ribosome profiling. Science *324*, 218–223.

Jalajakumari, M.B., Thomas, C.J., Halter, R., and Manning, P.A. (1989). Genes for biosynthesis and assembly of CS3 pili of CFA/II enterotoxigenic Escherichia coli: novel regulation of pilus production by bypassing an amber codon. Mol. Microbiol. *3*, 1685–1695.

Jungreis, I., Lin, M.F., Spokony, R., Chan, C.S., Negre, N., Victorsen, A., White, K.P., and Kellis, M. (2011). Evidence of abundant stop codon readthrough in Drosophila and other metazoa. Genome Res. *21*, 2096–2113.

Kamba, T., Tam, B.Y., Hashizume, H., Haskell, A., Sennino, B., Mancuso, M.R., Norberg, S.M., O'Brien, S.M., Davis, R.B., Gowen, L.C., et al. (2006). VEGF-dependent plasticity of fenestrated capillaries in the normal adult microvasculature. Am. J. Physiol. Heart Circ. Physiol. *290*, H560–H576.

Kim, D.H., Villeneuve, L.M., Morris, K.V., and Rossi, J.J. (2006). Argonaute-1 directs siRNA-mediated transcriptional gene silencing in human cells. Nat. Struct. Mol. Biol. *13*, 793–797.

Kisselev, L., Ehrenberg, M., and Frolova, L. (2003). Termination of translation: interplay of mRNA, rRNAs and release factors? EMBO J. *22*, 175–182.

Kondo, J., Francois, B., Urzhumtsev, A., and Westhof, E. (2005). Crystallographic studies of Homo sapiens ribosomal decoding A site complexed with aminoglycosides. Nucleic Acids Symp. Ser. (Oxf.), 253–254.

Konopatskaya, O., Churchill, A.J., Harper, S.J., Bates, D.O., and Gardiner, T.A. (2006). VEGF165b, an endogenous C-terminal splice variant of VEGF, inhibits retinal neovascularization in mice. Mol. Vis. *12*, 626–632.

Kristensen, A.R., Gsponer, J., and Foster, L.J. (2012). A high-throughput approach for measuring temporal changes in the interactome. Nat. Methods *9*, 907–909.

Lee, S., Chen, T.T., Barber, C.L., Jordan, M.C., Murdock, J., Desai, S., Ferrara, N., Nagy, A., Roos, K.P., and Iruela-Arispe, M.L. (2007). Autocrine VEGF signaling is required for vascular homeostasis. Cell *130*, 691–703.

Li, G.P., and Rice, C.M. (1989). Mutagenesis of the in-frame opal termination codon preceding nsP4 of Sindbis virus: studies of translational readthrough and its effect on virus replication. J. Virol. *63*, 1326–1337.

Low, S.C., and Berry, M.J. (1996). Knowing when not to stop: selenocysteine incorporation in eukaryotes. Trends Biochem. Sci. *21*, 203–208.

Manetti, M., Guiducci, S., Romano, E., Ceccarelli, C., Bellando-Randone, S., Conforti, M.L., Ibba-Manneschi, L., and Matucci-Cerinic, M. (2011). Overexpression of VEGF165b, an inhibitory splice variant of vascular endothelial growth factor, leads to insufficient angiogenesis in patients with systemic sclerosis. Circ. Res. *109*, e14–e26.

Mazumder, B., Sampath, P., Seshadri, V., Maitra, R.K., DiCorleto, P.E., and Fox, P.L. (2003). Regulated release of L13a from the 60S ribosomal subunit as a mechanism of transcript-specific translational control. Cell *115*, 187–198.

Miquerol, L., Langille, B.L., and Nagy, A. (2000). Embryonic development is disrupted by modest increases in vascular endothelial growth factor gene expression. Development *127*, 3941–3946.

Munro, T.P., Magee, R.J., Kidd, G.J., Carson, J.H., Barbarese, E., Smith, L.M., and Smith, R. (1999). Mutational analysis of a heterogeneous nuclear ribonucleoprotein A2 response element for RNA trafficking. J. Biol. Chem. *274*, 34389–34395.

Nagy, J.A., Dvorak, A.M., and Dvorak, H.F. (2007). VEGF-A and the induction of pathological angiogenesis. Annu. Rev. Pathol. *2*, 251–275.

Namy, O., Duchateau-Nguyen, G., Hatin, I., Hermann-Le Denmat, S., Termier, M., and Rousset, J.P. (2003). Identification of stop codon readthrough genes in Saccharomyces cerevisiae. Nucleic Acids Res. *31*, 2289–2296.

Pelham, H.R. (1978). Leaky UAG termination codon in tobacco mosaic virus RNA. Nature *272*, 469–471.

Poole, E.S., Brown, C.M., and Tate, W.P. (1995). The identity of the base following the stop codon determines the efficiency of in vivo translational termination in Escherichia coli. EMBO J. *14*, 151–158.

Qiu, Y., Bevan, H., Weeraperuma, S., Wratting, D., Murphy, D., Neal, C.R., Bates, D.O., and Harper, S.J. (2008). Mammary alveolar development during lactation is inhibited by the endogenous antiangiogenic growth factor isoform, VEGF165b. FASEB J. *22*, 1104–1112.

Rajon, E., and Masel, J. (2011). Evolution of molecular error rates and the consequences for evolvability. Proc. Natl. Acad. Sci. USA *108*, 1082–1087.

Ray, P.S., Jia, J., Yao, P., Majumder, M., Hatzoglou, M., and Fox, P.L. (2009). A stress-responsive RNA switch regulates VEGFA expression. Nature *457*, 915–919.

Rennel, E.S., Hamdollah-Zadeh, M.A., Wheatley, E.R., Magnussen, A., Schüler, Y., Kelly, S.P., Finucane, C., Ellison, D., Cebe-Suarez, S., Ballmer-Hofer, K., et al. (2008). Recombinant human VEGF165b protein is an effective anticancer agent in mice. Eur. J. Cancer *44*, 1883–1894.

Rennel, E.S., Varey, A.H., Churchill, A.J., Wheatley, E.R., Stewart, L., Mather, S., Bates, D.O., and Harper, S.J. (2009). VEGF(121)b, a new member of the VEGF(xxx)b family of VEGF-A splice isoforms, inhibits neovascularisation and tumour growth in vivo. Br. J. Cancer *101*, 1183–1193.

Robinson, D.N., and Cooley, L. (1997). Examination of the function of two kelch proteins generated by stop codon suppression. Development *124*, 1405–1417.

Sampath, P., Mazumder, B., Seshadri, V., Gerber, C.A., Chavatte, L., Kinter, M., Ting, S.M., Dignam, J.D., Kim, S., Driscoll, D.M., and Fox, P.L. (2004). Noncanonical function of glutamyl-prolyl-tRNA synthetase: gene-specific silencing of translation. Cell *119*, 195–208.

Schwartz, S.M., Haudenschild, C.C., and Eddy, E.M. (1978). Endothelial regeneration. I. Quantitative analysis of initial stages of endothelial regeneration in rat aortic intima. Lab. Invest. *38*, 568–580.

Senger, D.R., Galli, S.J., Dvorak, A.M., Perruzzi, C.A., Harvey, V.S., and Dvorak, H.F. (1983). Tumor cells secrete a vascular permeability factor that promotes accumulation of ascites fluid. Science *219*, 983–985.

Shan, J., Munro, T.P., Barbarese, E., Carson, J.H., and Smith, R. (2003). A molecular mechanism for mRNA trafficking in neuronal dendrites. J. Neurosci. *23*, 8859–8866.

Shih, S.C., and Claffey, K.P. (1999). Regulation of human vascular endothelial growth factor mRNA stability in hypoxia by heterogeneous nuclear ribonucleoprotein L. J. Biol. Chem. *274*, 1359–1365.

Soker, S., Takashima, S., Miao, H.Q., Neufeld, G., and Klagsbrun, M. (1998). Neuropilin-1 is expressed by endothelial and tumor cells as an isoform-specific receptor for vascular endothelial growth factor. Cell *92*, 735–745.

Steneberg, P., and Samakovlis, C. (2001). A novel stop codon readthrough mechanism produces functional Headcase protein in Drosophila trachea. EMBO Rep. *2*, 593–597.

Tate, W.P., Mansell, J.B., Mannering, S.A., Irvine, J.H., Major, L.L., and Wilson, D.N. (1999). UGA: a dual signal for 'stop' and for recoding in protein synthesis. Biochemistry (Mosc.) *64*, 1342–1353.

Turanov, A.A., Xu, X.M., Carlson, B.A., Yoo, M.H., Gladyshev, V.N., and Hatfield, D.L. (2011). Biosynthesis of selenocysteine, the 21st amino acid in the genetic code, and a novel pathway for cysteine biosynthesis. Adv. Nutr. *2*, 122–128.

Varey, A.H., Rennel, E.S., Qiu, Y., Bevan, H.S., Perrin, R.M., Raffy, S., Dixon, A.R., Paraskeva, C., Zaccheo, O., Hassan, A.B., et al. (2008).

VEGF 165 b, an antiangiogenic VEGF-A isoform, binds and inhibits bevacizumab treatment in experimental colorectal carcinoma: balance of pro- and antiangiogenic VEGF-A isoforms has implications for therapy. Br. J. Cancer *98*, 1366–1379.

von der Haar, T., and Tuite, M.F. (2007). Regulated translational bypass of stop codons in yeast. Trends Microbiol. *15*, 78–86.

Woolard, J., Wang, W.Y., Bevan, H.S., Qiu, Y., Morbidelli, L., Pritchard-Jones, R.O., Cui, T.G., Sugiono, M., Waine, E., Perrin, R., et al. (2004). VEGF165b, an inhibitory vascular endothelial growth factor splice variant: mechanism of action, in vivo effect on angiogenesis and endogenous protein expression. Cancer Res. *64*, 7822–7835.

Yamaguchi, Y., Hayashi, A., Campagnoni, C.W., Kimura, A., Inuzuka, T., and Baba, H. (2012). L-MPZ, a novel isoform of myelin P0, is produced by stop codon readthrough. J. Biol. Chem. *287*, 17765–17776.

Yao, P., Potdar, A.A., Arif, A., Ray, P.S., Mukhopadhyay, R., Willard, B., Xu, Y., Yan, J., Saidel, G.M., and Fox, P.L. (2012). Coding region polyadenylation generates a truncated tRNA synthetase that counters translation repression. Cell *149*, 88–100.

Zaltsman, Y., Shachnai, L., Yivgi-Ohana, N., Schwarz, M., Maryanovich, M., Houtkooper, R.H., Vaz, F.M., De Leonardis, F., Fiermonte, G., Palmieri, F., et al. (2010). MTCH2/MIMP is a major facilitator of tBID recruitment to mitochondria. Nat. Cell Biol. *12*, 553–562.

Cell

EXTENDED EXPERIMENTAL PROCEDURES

Antibodies

Polyclonal anti-VEGF-Ax antibody was generated by injecting into rabbits synthetic KLH-conjugated peptide, AGLEEGASLRVSGTR; the same peptide was used for affinity purification. Anti-hnRNP A2/B1 was from Abcam (for immunofluorescence microscopy) or from Santa Cruz (clone EF-67, for immunoprecipitation and immunoblot analysis). Anti-VEGF-A (N terminus), neutralizing anti-VEGF-A (clone JH121), and horseradish peroxidase-conjugated secondary antibodies were from Thermo Fisher; anti-VEGF-Ab was from R&D; anti-Myc-tag, anti-phospho VEGFR2 and anti-VEGFR2 antibodies were from Cell Signaling; anti-GAPDH and anti-α-tubulin were from Sigma; anti-HDAC-1 was from BioVision; IgG from Santa Cruz, and Alexa Fluor-conjugated secondary antibody was from Molecular Probes.

Cell Migration

Cell migration was measured by razor-wound method. Confluent bovine aortic EC cultures maintained in serum-free medium for 24 hr were wounded by gently pressing a razor through the cell layer to mark the wound line and then drawn through the monolayer to remove cells on one side of the line. Migration was allowed for 24 hr in serum-free medium containing 1 mg/ml of bovine serum albumin and IgG or anti-VEGF-A or -VEGF-Ax antibodies (5 μg/ml) or His-VEGF-Ax^{Ala} (50 ng/ml). Following fixation and staining with Giemsa-Wright (Sigma), cells crossing the wound line at two randomly chosen regions 1.5 mm in length were counted by a semi-automated, computer-assisted procedure. To calculate root-mean-square displacement and speed, cells were imaged every 5 min for 1,000 min by a phase-contrast microscope (Leica) equipped with temperature-controlled humidified chamber and motorized x-y stage. Migrating cells were subjected to automatic tracking using ''track objects'' function in Metamorph and *x*- and *y*-coordinates were acquired. All cell migration experiments were analyzed by a person blinded to the treatments.

Cell Proliferation

Bovine aortic ECs were allowed to attach for 4 hr in 96-well plates (~10,000 cells/well) and medium replaced with Opti-MEM (Invitrogen) containing IgG, or anti-VEGF-A or anti-VEGF-Ax antibodies (5 μg/ml), recombinant VEGF-A (R&D Systems, 20 ng/ml), or His-VEGF-Ax^{Ala} (50 ng/ml). Total cell DNA was determined fluorometrically using CyQUANT NF Cell Proliferation Assay Kit (Invitrogen) with excitation at 485 nm and emission at 538 nm (Spectramax Gemini EM).

Immunoblot Analysis

Cell lysates or conditioned media were denatured and resolved on 4%–20% gradient SDS-PAGE. To differentiate canonical VEGF-A and VEGF-Ax on same gel, lysates or conditioned media were subjected to protein deglycosylation mix (New England Biolabs) and resolved on 16% Tricine gel (Invitrogen). After transfer, the blots were probed with specific primary antibody followed by HRP-conjugated secondary antibody, and developed using ECL or ECL plus reagent (GE Healthcare). Nuclear and cytoplasmic fractions were isolated using NE-PER reagent (Thermo Scientific).

Mass Spectrometry

Bovine $VEGFA_{164}$ cDNA and the Ax element were cloned in a construct containing an in-frame polyHis-tag. The downstream stop codon was excluded so that readthrough at the canonical stop codon generated a polyHis-tagged chimeric protein. Serum-free conditioned medium was obtained from stably transfected HEK293 cells. His-tagged readthrough product was purified using Ni-NTA agarose (QIAGEN) and subjected to SDS-PAGE electrophoresis. An about 28 kDa band was cut from the gel stained with Imperial protein stain (Thermo Scientific), digested with trypsin, and analyzed by capillary column LC-MS/MS (LTQ-Orbitrap Elite system coupled to a Dionex Ultimate 3000 HPLC fitted with a 15 cm x 75 μm i.d. Acclaim Pepmap C18 reverse-phase capillary column). Peptides were eluted using 0.5% formic acid and 95% acetonitrile mobile phases at a flow rate of 0.3 μl/min. The digest was analyzed in survey and targeted modes. Survey experiments were done using the data-dependent multitask capability of the instrument acquiring full scan mass spectra to interrogate peptide molecular weights and product ion spectra to determine amino acid sequence in successive instrument scans. The data were analyzed by Mascot using all collected CID spectra to search the bovine reference sequence database. The targeted selective reaction monitoring (SRM) experiments involved fragmentation of specific readthrough peptides over the entire course of the LC experiment.

siRNAs

VEGF-A-specific siRNAs target the following sequences in bovine *VEGFA* mRNA:

siRNA 1, 5′ GCTTCCTACAGCATAACAAATGTGA 3′
siRNA 2, 5′ GGAGTACCCAGATGAGATT 3′
siRNA 3, 5′ ATGTGAATGCAGACCAAAG 3′

hnRNP A2/B1-specific siRNA targets the following sequence in bovine *HNRNPA2/B1* mRNA: 5′ GGCTTTGTCTAGACAAGAAAT GCAG 3′.

All siRNAs were transfected using Lipofectamine 2000 and expression of target genes determined after 3 days by immunoblot analysis.

Immunoprecipitation and RNA-Binding Protein Immunoprecipitation

Cell extracts were precleared with protein A-Sepharose beads and IgG for 1 hr at 4°C. Antibody was added and samples tumbled overnight at 4°C. Immune complexes bound to protein A-Sepharose beads were isolated by centrifugation followed by extensive washing. For immunoprecipitation, protein was extracted using Laemmli buffer. For RIP analysis, RNA bound to immune complexes was isolated by RNeasy Mini Kit (QIAGEN).

VEGFA Sequencing

Total RNA was isolated from bovine ECs using RNeasy Mini Kit (QIAGEN). *VEGFA* cDNA was generated by reverse transcription followed by PCR using SuperScript III One-Step RT-PCR System (Invitrogen). Primers used were:

Forward, 5′ ATGCAAGCTTATGAACTTTCTGCTCTCTTGGG 3′ Reverse, 5′ ATGCGGATCCGTCTTTCCTGGTGAGACGTCT 3′

cDNAs were cloned in pGEM-T vector and subjected to capillary sequencing using T7 Universal-R1 primer: 5′ TAATACGACTCAC TATAGG 3′.

RT-PCR Analysis

Total bovine EC RNA, or RNA isolated from RIP samples, were subjected to reverse transcription and real-time PCR using AgPath-ID One-Step RT-PCR reagent (Ambion). Firefly *luciferase (FLuc)*-, bovine *VEGFA*- and *GAPDH*-specific TaqMan probes (Applied Biosystems) were used. *FLuc* and *VEGFA* mRNA levels were normalized by *GAPDH* mRNA. In RIP experiments, hnRNP A2/B1-bound *FLuc* mRNA was quantified relative to the *FLuc* mRNA in input samples. Following *VEGFA*-specific primers were used for PCR to differentiate between antiangiogenic *VEGF-Ab* isoforms and proangiogenic *VEGF-A* isoforms:

Forward, 5′ ATGCGGATCAAACCTCACC 3′

Reverse, 5′ GTCTTTCCTGGTGAGACG 3′

Plasmid Construction

pcDNA 3.1 (Invitrogen) was the backbone vector for all constructs. Bovine $VEGFA_{164}$ cDNA from ECs was cloned with the Ax element in HindIII and BamHI sites. The canonical stop codon separating VEGF-A_{164} coding sequence from Ax element was retained, but the downstream in-frame stop codon was omitted. Firefly luciferase (*FLuc*) was cloned without its start codon (ATG) between BamHI and NotI. The following linker sequence was added at the 5′ end of *FLuc*: 5′ GGCGGCTCCGGCGGCTCCCTCGTGCTCGAG 3′. In a separate construct, *Myc* replaced VEGF-A_{164}. In all constructs, *FLuc* was in-frame with $VEGFA_{164}$ or *Myc*. Mutations were done using GeneArt Site-Directed Mutagenesis System (Invitrogen). To test candidate genes for translational readthrough, ~700 nt at the 3′ end of human coding sequences (*TOX*, 684 nt; *ADAMTS4*, 741 nt; *AGO1*, 696 nt; *NR1D1*, 669 nt; *MTCH2*, 732 nt) were cloned with interstop codon regions upstream to and in-frame with *FLuc*. Authenticity of all constructs was confirmed by sequencing.

Surface Plasmon Resonance Analysis of Protein-RNA Binding

Biotinylated RNA (5′ Bio-UGUGACAAGCCGAGGCGGUGAGCCGGGCAGGAGGAAGGAGCCUC 3′) containing the putative A2RE of *VEGFA* mRNA (Dharmacon) was immobilized on a streptavidin sensor chip in a BIAcore 3000 (GE Healthcare). Recombinant human hnRNP A2/B1 (Abnova) was injected at 20 μl/min for 3 min in a running buffer of 10 mM HEPES (pH 7.4), 150 mM NaCl and 0.005% Surfactant P20, and cells were regenerated using 50 mM NaOH. K_D were calculated using Biaevaluation software.

Expression and Purification of His-VEGF-Ax^{Ala}

HEK293-6E cells were cultured in serum-free Freestyle 293 expression medium (Invitrogen) and transfected with vector pTT5 expressing His-VEGF-Ax^{Ala} using PEI (Polysciences); the canonical TGA stop codon was mutated to GCA to ensure robust synthesis of VEGF-Ax-like protein. His-VEGF-Ax^{Ala} was purified from conditioned medium collected 6 days after transfection using HisTrap FF crude column (GE Healthcare). Purified His-VEGF-Ax^{Ala} was detected with anti-VEGF-Ax, anti-VEGF-Ab and anti-VEGFA antibodies.

Solid-Phase Enzyme-Linked Receptor-Binding Assay

Maxisorp 96-well plates (Nunc) were coated with 3 μg/ml of VEGFR2 (R&D Systems) in Tris-buffered saline (TBS) at 4°C overnight. Wells were blocked in 5% milk in TBS for 1 hr followed by incubation with serial dilutions of ligands for 2 hr, and then with anti-VEGF-A antibody for 2 hr. HRP-conjugated secondary antibody was added for 1 hr and color developed with 3,3′,5,5′-tetramethylbenzidine (TMB, Pierce). The reaction was stopped by addition of 1 N HCl, and absorption at 450 nm was measured using a microplate reader (SpectraMax 190, Molecular Devices). All washes were done with TBS containing 0.05% Tween 20. For binding to neuropilin-1, a similar protocol was followed except phosphate-buffered saline (PBS) was used in place of TBS, 0.5% BSA was used in place of 5% milk, and 2 μg/ml of heparin was added with ligand.

VEGFR2 Phosphorylation Studies

HUVECs were cultured in serum-free OptiMem medium for 4 hr, followed by treatment with VEGF-A (20 ng/ml) or VEGF-Ax (50 ng/ml) for up to 30 min. Cells were lysed using PhosphoSafe extraction reagent (EMD Millipore) and resolved on 7.5% SDS-PAGE. After transfer, blots were probed with anti-phospho-VEGFR2 and anti-VEGFR2 antibodies.

Fluorescence Microscopy

Tissue arrays contained 1.5-mm by 5-μm thick samples (US Biomax). The adenocarcinoma array contained samples from 30 cases and 5 healthy individuals. Sections were deparaffinized, rehydrated, and subjected to antigen retrieval using Target retrieval solution (Dako) at 95°C for 25 min. Sections were blocked with 5% horse serum for 2 hr, incubated with anti-VEGF-A or -VEGF-Ax antibodies, or IgG overnight at 4°C, and then stained with Alexa Fluor 488-conjugated secondary antibody at room temperature for 1 hr. Fluorescence intensity was quantified using NIH ImageJ software, and background fluorescence from IgG samples was subtracted. Frozen human tissue sections were fixed with 4% paraformaldehyde in PBS, permeabilized with 0.1% Triton X-100, and incubated with anti-VEGF-Ax antibody followed by Alexa Fluor 488-conjugated secondary antibody. The same protocol was used to image hnRNP A2/B1 in cultured ECs. Single-plane, confocal images were obtained with a 1.0 Airy pinhole (Leica DMRXE with confocal TCS SP2 unit).

Endothelial Cell Tube Formation

Bovine aortic ECs were pretreated with 50 ng/ml of His-VEGF-Ax^{Ala} for 6 hr after which they were (10^5 cells/cm^2) seeded on growth factor-reduced LDEV-free Matrigel (BD Biosciences) on μ-slides developed for angiogenesis assays (Ibidi). Incubation with His-VEGF-Ax^{Ala} was continued for 10 hr. Cells were then fixed with 4% paraformaldehyde, stained with CyQUANT dye and imaged. Total tube length was quantified using ImageJ.

Genome-wide Analysis of Readthrough

3′UTRs from *H. sapiens*, *M. mulatta*, *B. taurus*, *M. musculus*, and *R. norvegicus* were retrieved from a UTR database (http://utrdb.ba.itb.cnr.it/). 3′UTR sequences from 6,357 genes common to the five species were translated in silico using BioPerl translate module. The 5′-most 60-amino acid sequence of each 3′UTR were aligned and scored. Using a cut-off of 1,400, heuristically chosen to include scores > 70% of *VEGFA* score, 539 genes were selected for manual screening; mRNAs that undergo alternative splicing at the 3′UTR, lack downstream, in-frame stop codons, or exhibit conservation after the downstream stop codon were removed.

Statistics

Unless mentioned otherwise Student's t test was employed to test the significance of differences we observed in various experiments. Mann-Whitney test was used for the analysis of VEGF-A isoform expression in colon tissues.

A

ATGAACTTTCTGCTCTCTTGGGTACATTGGAGCCTTGCCTTGCTGCTCTACCTTCACCATGCCAAGTGGTCCCAGGCTGCA
CCCATGGCAGAAGGAGGGCAGAAACCCCACGAAGTGGTGAAGTTCATGGATGTCTACCAGCGCAGCTTCTGCCGTCCCATC
GAGACCCTGGTGGACATCTTCCAGGAGTACCCAGATGAGATTGAGTTCATTTTCAAGCCGTCCTGTGTGCCCCTGATGCGG
TGCGGGGGCTGCTGTAATGACGAAAGTCTGGAGTGTGTGCCCACTGAGGAGTTCAACATCACCATGCAGATTATGCGGATC
AAACCTCACCAAAGCCAGCACATAGGAGAGATGAGCTTCCTACAGCATAACAAATGTGAATGCAGACCAAAGAAAGATAAA
GCAAGGCAAGAAAATCCCTGTGGGCCTTGCTCAGAGCGGAGAAAGCATTTGTTTGTACAAGATCCGCAGACGTGTAAATGT
TCCTGCAAAAACACAGACTCGCGTTGCAAGGCGAGGCAGCTTGAGTTAAACGAACGTACTTGCAGATGTGACAAGCCGAGG
CGGTGAGCCGGGCTGGAGGAAGGAGCCTCCCTCAGGGTTTCGGGAACCAGACGTCTCACCAGGAAAGACTGA

Expected MW of readthrough product: 20.46 kDa (after signal peptide cleavage)

B

ATGAACTTTCTGCTCTCTTGGGTACATTGGAGCCTTGCCTTGCTGCTCTACCTTCACCATGCCAAGTGGTCCCAGGCTGCA
CCCATGGCAGAAGGAGGGCAGAAACCCCACGAAGTGGTGAAGTTCATGGATGTCTACCAGCGCAGCTTCTGCCGTCCCATC
GAGACCCTGGTGGACATCTTCCAGGAGTACCCAGATGAGATTGAGTTCATTTTCAAGCCGTCCTGTGTGCCCCTGATGCGG
TGCGGGGGCTGCTGTAATGACGAAAGTCTGGAGTGTGTGCCCACTGAGGAGTTCAACATCACCATGCAGATTATGCGGATC
AAACCTCACCAAAGCCAGCACATAGGAGAGATGAGCTTCCTACAGCATAACAAATGTGAATGCAGACCAAAGAAAGATAAA
GCAAGGCAAGAAAAATGTGACAAGCCGAGGCGGTGAGCCGGGCTGGAGGAAGGAGCCTCCCTCAGGGTTTCGGGAACCAGA
CGTCTCACCAGGAAAGACTGA

Expected MW of readthrough product: 15.62 kDa (after signal peptide cleavage)

C

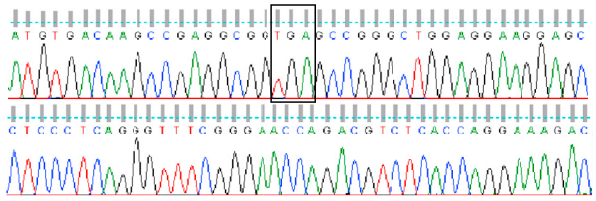

D

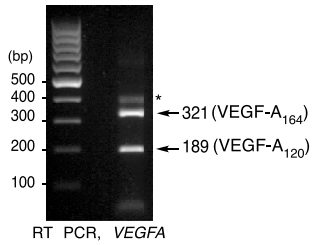

E

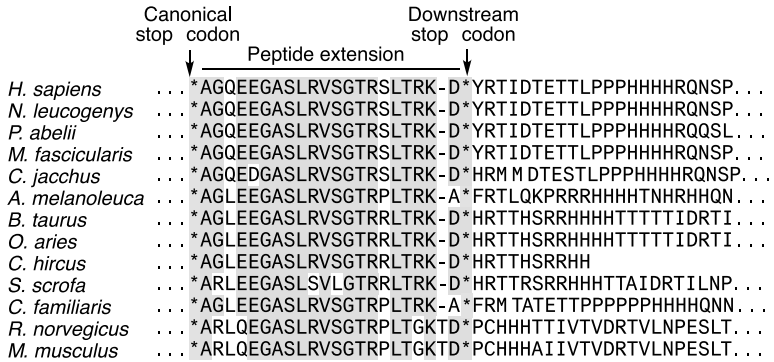

F

	Sequence conservation		
Species comparison	Coding sequence	Peptide extension	Downstream 3' UTR (66 nt after distal stop codon)
H. sapiens vs. *B. taurus*	95%	91%	9%
B. taurus vs. *M. musculus*	89%	78%	9%
H. sapiens vs. *M. musculus*	90%	74%	5%

Figure S1. *VEGFA* Isoform Sequences and Conservation, Related to Figure 1

(A and B) VEGF-A_{164} (A) and VEGF-A_{120} (B) nucleotide sequences expressed in bovine aortic ECs. Cleaved signal peptide is indicated (gray background).

(C) Electropherogram of *VEGFA* cDNA sequence from bovine aortic EC. Distal part of coding sequence and region between the canonical stop codon (in box) and downstream stop codon.

(D) Absence of VEGF-Ab mRNA isoforms in ECs. RNA isolated from bovine aortic ECs was subjected to reverse transcription followed by PCR (35 cycles). Primers were designed so that alternatively spliced VEGF-Ab isoforms would generate 273- and 141-bp products, and isoforms not spliced in this region (exon 8) would give 321- and 189-bp products; nonspecific band (*).

(E) Multiple sequence alignment of amino acids potentially encoded by the region between two in-frame stop codons in mammalian *VEGFA* 3′UTR. Conserved sequences are highlighted (gray background).

(F) Comparison of sequence conservation. Sequence conservation (amino acid identity, %) in the coding sequence, the peptide extension between the two stop codons (Ax element), and the region 66 nt downstream of the distal stop codon is shown.

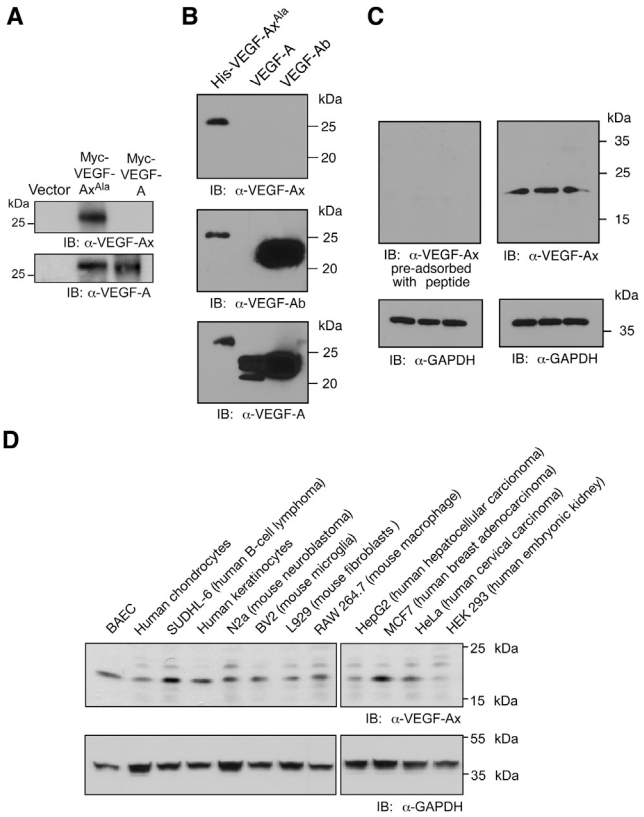

Figure S2. Specificity of Anti-VEGF-Ax Antibody, Related to Figure 2

(A) Anti-VEGF-Ax antibody recognizes VEGF-Ax, but not VEGF-A. HEK293 cells were transfected with Myc-tagged *VEGFA* cDNA in which the canonical stop codon is mutated to GCA (VEGF-Ax^{Ala}), or with Myc-tagged *VEGFA* cDNA, and conditioned media subjected to immunoblot analysis with anti-VEGF-Ax and -VEGF-A antibodies.

(B) Anti-VEGF-Ax antibody does not recognize VEGF-A or VEGF-Ab. Recombinant His-VEGF-Ax^{Ala}, VEGF-A, and VEGF-Ab were immunoblotted with anti-VEGF-Ax, anti-VEGF-Ab and anti-VEGF-A antibodies.

(C) Confirmation of anti-VEGF-Ax specificity. EC lysates were pre-adsorbed with AGLEEGASLRVSGTR peptide (1 μg/ml overnight at 4°C) and immunoblotted with anti-VEGF-Ax antibody.

(D) VEGF-Ax is expressed in multiple cell types. Lysates from multiple cell types were immunoblotted with anti-VEGF-Ax and anti-GAPDH antibodies.

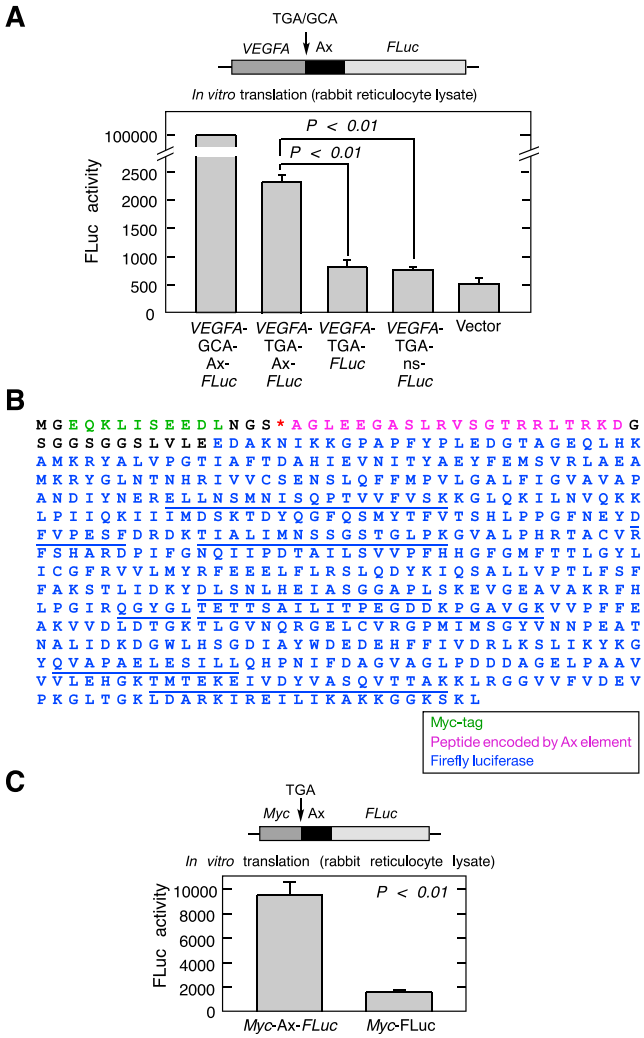

Figure S3. Ax-Dependent Readthrough In Vitro Using Rabbit Reticulocyte Lysate and Readthrough of Heterologous Transcript, Related to Figure 3

(A) Ax-dependent readthrough in vitro. Plasmids containing in-frame *VEGF*-Ax-*FLuc*, and variants with TGA-to-GCA substitution, no Ax element, and Ax replaced by a nonspecific sequence (ns), were subjected to in vitro coupled transcription-translation using rabbit reticulocyte lysate, and FLuc activity of the products measured.

(B) Mass spectrometric analysis of readthrough of heterologous transcript. ECs were transfected with plasmid containing *Myc-Ax-FLuc* and lysate subjected to immunoprecipitation using anti-Myc-tag antibody. The precipitate was resolved in SDS-PAGE, the ~66 kDa band subjected to MS analysis; identified FLuc peptides are highlighted (underline).

(C) Ax-dependent readthrough of heterologous transcript in vitro. Chimeric plasmids containing *Myc*-Ax-*FLuc* and *Myc-FLuc* were subjected to in vitro coupled transcription-translation using rabbit reticulocyte lysate, and FLuc activity measured.

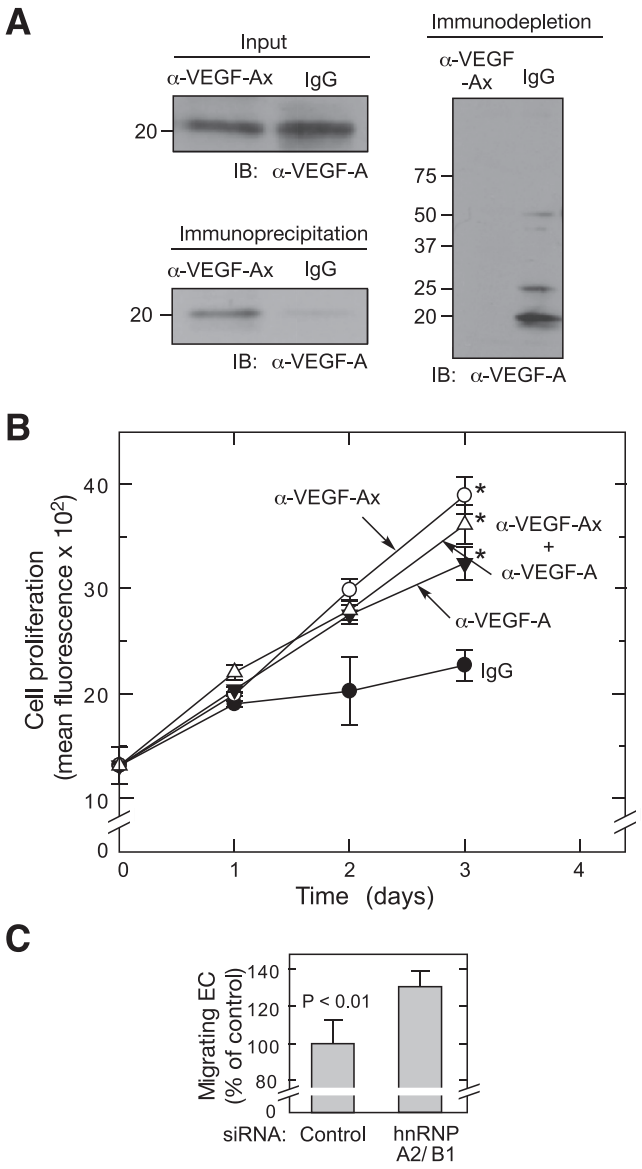

Figure S4. VEGF-Ax in BAEC Conditioned Medium and Migration of hnRNP A2/B1 Knockdown BAECs, Related to Figure 5

(A) Conditioned medium derived from BAECs grown in serum-free medium without any growth factors was concentrated and subjected to immunodepletion using anti-VEGF-Ax antibody. Immunodepleted samples and immunoprecipitants were resolved on SDS-PAGE and probed with anti-VEGF-A antibody.

(B) Effect of VEGF-Ax inhibition on EC proliferation. ECs were treated with antibodies indicated and cell proliferation quantified using CyQUANT NF Cell Proliferation Assay Kit (*$p < 0.01$, 2-way ANOVA).

(C) Migration of hnRNP A2/B1 knockdown BAECs.

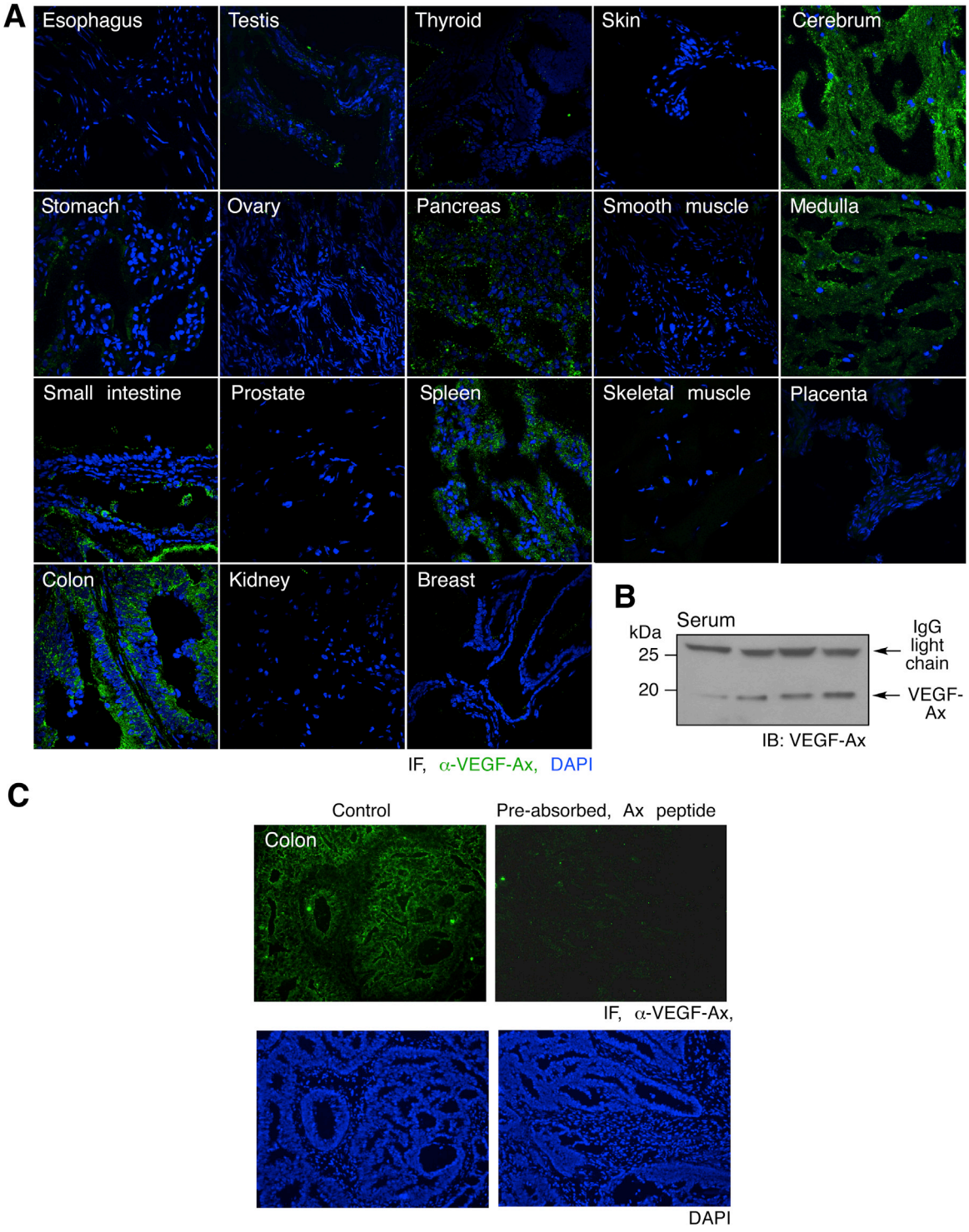

Figure S5. In Vivo Expression of VEGF-Ax, Related to Figure 6

(A) VEGF-Ax expression in human tissues. Microarray sections of frozen human tissues were subjected to immunofluorescence with anti-VEGF-Ax antibody followed by Alexa Fluor 488-conjugated secondary antibody, and DAPI stain, and imaged by confocal microscopy.

(B) VEGF-Ax expression in human serum. Serum from healthy subjects (n = 4) was subjected to immunoblot analysis with anti-VEGF-Ax antibody.

(C) Validation of anti-VEGF-Ax antibody for immunofluorescence. Frozen colon tissue sections were stained with anti-VEGF-Ax antibody and DAPI before and after preadsorption with AGLEEGASLRVSGTR (1 μg/ml overnight at 4°C), and imaged by immunofluorescence microscope.

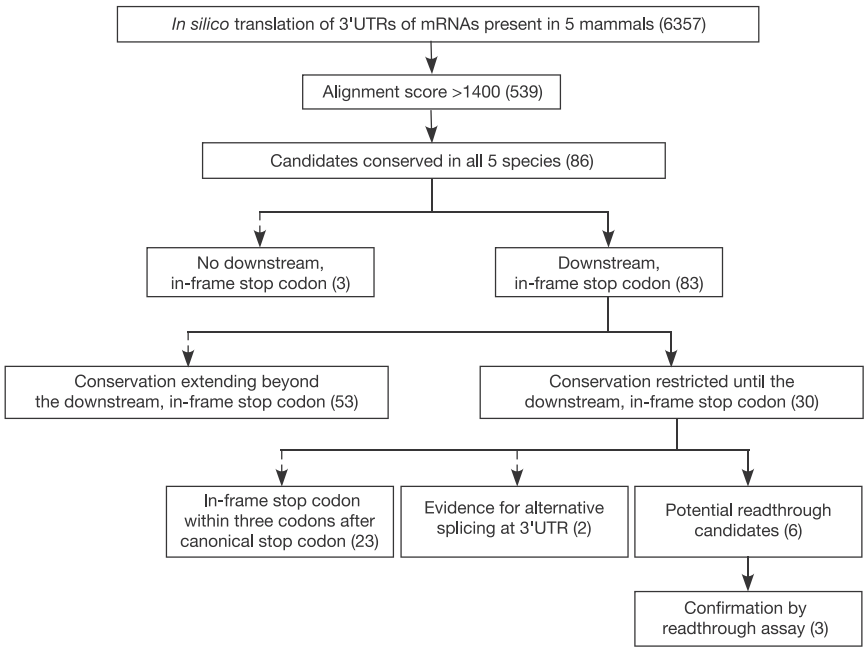

Figure S6. Genome-wide Analysis of Translational Readthrough Targets, Related to Figure 7
Flow chart of bioinformatic screen employed to identify readthrough candidates.